OPEN ACCESS Freely available online

PLOS ONE

Expression of Signaling Components in Embryonic Eyelid Epithelium

Qinghang Meng, Chang Jin, Yinglei Chen, Jing Chen, Mario Medvedovic, Ying Xia*

Department of Environmental Health, College of Medicine, University of Cincinnati, Cincinnati, Ohio, United States of America

Abstract

Closure of an epithelium opening is a critical morphogenetic event for development. An excellent example for this process is the transient closure of embryonic eyelid. Eyelid closure requires shape change and migration of epithelial cells at the tip of the developing eyelids, and is dictated by numerous signaling pathways. Here we evaluated gene expression in epithelial cells isolated from the tip (leading edge, LE) and inner surface epithelium (IE) of the eyelid from E15.5 mouse fetuses by laser capture microdissection (LCM). We showed that the LE and IE cells are different at E15.5, such that IE had higher expression of muscle specific genes, while LE acquired epithelium identities. Despite their distinct destinies, these cells were overall similar in expression of signaling components for the "eyelid closure pathways". However, while the LE cells had more abundant expression of *Fgfr2*, *Erbb2*, *Shh*, *Ptch1* and *2*, *Smo* and *Gli2*, and *Jag1* and *Notch1*, the IE cells had more abundant expression of *Bmp5* and *Bmpr1a*. In addition, the LE cells had more abundant expression of *adenomatosis polyposis coli down-regulated 1* (*Apcdd1*), but the IE cells had high expression of *Dkk2*. Our results suggest that the functionally distinct LE and IE cells have also differential expression of signaling molecules that may contribute to the cell-specific responses to morphogenetic signals. The expression pattern suggests that the EGF, Shh and NOTCH pathways are preferentially active in LE cells, the BMP pathways are effective in IE cells, and the Wnt pathway may be repressed in LE and IE cells via different mechanisms.

Citation: Meng Q, Jin C, Chen Y, Chen J, Medvedovic M, et al. (2014) Expression of Signaling Components in Embryonic Eyelid Epithelium. PLoS ONE 9(2): e87038. doi:10.1371/journal.pone.0087038

Editor: Fu-Shin Yu, Wayne State University, United States of America

Received July 11, 2013; **Accepted** November 7, 2013; **Published** February 3, 2014

Funding: This work is supported in part by funding from National Institutes of Health, National Eye Institute R01EY15227 and National Institute of Environmental Health Sciences P30 ES006096. The funders had no role in study design, data collection and analysis, decision to publish, or preparation of the manuscript.

Competing Interests: The authors have declared that no competing interests exist.

* E-mail: ying.xia@uc.edu

Introduction

Formation of the eyelid is one of the last major morphogenetic events in mammalian prenatal development. Though for the most part data are scarce in humans, histological analyses of available embryos/fetuses have shown that eyelid development proceeds through four distinct phases, namely, lid formation, growth, fusion and re-opening [1,2]. In mice, eyelid development follows similar steps but has been characterized in greater detail. Mouse eyelid formation begins at around embryonic day 11.5 (E11.5). At this time, the surface ectoderm adjacent to the developing cornea folds to form the lid buds, which are a simple structure consisting of loose periocular mesenchyme (POM) covered by undifferentiated ectoderm [3–6]. The eyelid buds grow from E12 onward, and they extend across the ocular surface, undergoing proliferation and differentiation. The eyelid at this stage is covered by epidermis, overlaid by periderm at the anterior surface and conjunctiva at the posterior surface. The epithelial margins of the superior and inferior lid fuse between E15 - E16. Lid fusion begins when the periderm cells become rounded and piled up at the leading edges of the eyelids, and then stream out across the corneal surface. The eyelids meet at the inner and outer canthi and temporarily fuse across the cornea [3,4]. Once contact is established between the apposed eyelids, the cells at the fusion junction flatten and form a strip along the fusion line, and they slough off with the rest of the periderm [4,7,8]. Mouse eyelid remains closed between E16.5 and postnatal day 12–14. Cells at the eyelid fusion junction undergo desquamation and/or apoptosis, resulting in separation of the upper and lower eyelids at around postnatal day 14 [4,9].

Much is known about the molecular factors involved in eyelid formation and fusion. This is because, although mice are normally born with a closed eyelid, a large number of genetic mutant strains display a distinct "eye open at birth" (EOB) phenotype. The Mouse Genome Informatics (MGI) (http://www.informatics.jax.org/) has a collection of >138 genotypes associated with the phenotype; the number is likely to increase with complete or partial knockout of new genes.

The majority of the EOB phenotype is caused by failure of eyelid fusion at E15–E16. One of the most significant findings made by the analysis of EOB mice is that multiple signaling pathways are involved in the regulation of eyelid closure. Some pathways, such as RA-RXR/RAR and PITX2-DKK2, and the FOXL and OAR2 transcription factors, seem to operate in the periocular mesenchyme [10–12]; others, such as the FGF10-FGFR and BMP-BMPR pathways, act through crosstalk between mesenchyme and epithelium [6,13]. Furthermore, a number of pathways, including MAP3K1-JNK, EGFR, ROCK and PCP, are specifically effective in the eyelid epithelial cells [14–35]. There is also evidence for signal compartmentalization and spatial segregation, so that the signaling pathways are activated in distinct cell population in the developing eyelids [21,36].

Though the outline of the pathways is more or less drawn, the role that the actual players involved in signal transduction has not

Table 1. Gene Functions in LE and IE Cells.

categoryID	description	nGenes	zScore	pValue	FDR
Up-regulated in LE cells					
GO:0008544	epidermis development	202	9.513937667	9.18E-22	4.91E-18
GO:0001071	nucleic acid binding transcription factor activity	725	7.756885322	4.35E-15	7.76E-12
GO:0007389	pattern specification process	389	6.372488177	9.30E-11	6.78E-08
GO:0042475	odontogenesis of dentin-containing tooth	56	6.359209662	1.01E-10	6.78E-08
Up-regulated in IE cells					
GO:0005865	striated muscle thin filament	15	9.710632193	1.35823E-22	7.26656E-19
GO:0008380	RNA splicing	222	7.022839172	1.08702E-12	2.90778E-09
GO:0005815	microtubule organizing center	353	5.980688777	1.11098E-09	8.49106E-07
GO:0005813	centrosome	334	5.947685008	1.35981E-09	9.09371E-07

doi:10.1371/journal.pone.0087038.t001

Table 2. Expression of Genes in the FGF pathways

		LE		IE		LE/IE	
symbol	**name**	**ave.int**	**p-value**	**ave.int**	**p-value**	**fold**	**p.value**
The FGF family							
Ligands							
Fgf9	fibroblast growth factor 9	**391.7362245**	**0.002337928**	**390.6433611**	**0.019267398**	1.002797599	0.240347549
Fgf8	fibroblast growth factor 8	166.5464506	0.155681338	168.861405	0.535466303	-1.013899752	0.2104111
Fgf22	fibroblast growth factor 22	126.5957788	0.368634212	159.4079042	0.616024893	-1.259188147	0.291215529
Fgf17	fibroblast growth factor 17	125.059223	0.381111278	120.5839736	0.943298623	1.037113136	0.142005947
Fgf15	fibroblast growth factor 15	106.552639	0.567451803	196.9766114	0.349464154	-1.848631936	0.423612008
Fgf18	fibroblast growth factor 18	100.7913239	0.641017588	210.65336	0.283116505	-2.08999497	0.519448518
Fgf13	fibroblast growth factor 13	89.66438499	0.807082058	189.7867092	0.390149852	-2.11663426	0.303068764
Fgf23	fibroblast growth factor 23	87.28123282	0.846919936	129.6743787	0.937844546	-1.48570746	0.083917121
Fgf12	fibroblast growth factor 12	85.02659868	0.886003145	165.5686431	0.562397439	-1.947257043	0.183738989
Fgf14	fibroblast growth factor 14	81.91780637	0.942085876	151.3383997	0.692901632	-1.847442045	0.860187995
Fgf4	fibroblast growth factor 4	77.78685355	0.979586236	99.0757551	0.635380846	-1.273682513	0.229425806
Fgf2	fibroblast growth factor 2	70.66744472	0.835369348	217.5071721	0.254690818	-3.077897793	0.13672465
Fgf3	fibroblast growth factor 3	68.74815066	0.794789854	90.72130986	0.512539018	-1.319618186	0.335560338
Fgf11	fibroblast growth factor 11	68.56522928	0.790890829	75.35099222	0.300332225	-1.09896799	0.170136214
Fgf20	fibroblast growth factor 20	66.76075364	0.752163879	108.3953639	0.772018719	-1.623639009	0.832224495
Fgf5	fibroblast growth factor 5	56.66072417	0.53052365	83.88846438	0.414768503	-1.480539926	0.545076451
Fgf6	fibroblast growth factor 6	56.09740044	0.518165165	61.21500656	0.14375436	-1.091227153	0.004820016
Fgf1	fibroblast growth factor 1	50.52878074	0.39830177	66.54665181	0.196832397	-1.3170049	0.871058322
Fgf16	fibroblast growth factor 16	46.44946676	0.315151851	83.9707348	0.415920032	-1.807786842	0.213019604
Fgf21	fibroblast growth factor 21	43.45787888	0.258114299	80.28778119	0.365183695	-1.847485042	0.47884619
Fgf7	fibroblast growth factor 7	40.01974398	0.197978384	177.3818719	0.47111134	-4.432358986	0.137301471
Fgf10	fibroblast growth factor 10	39.45348786	0.188715937	62.20935837	0.153034151	-1.576777156	NA
Receptors							
Fgfr2	fibroblast growth factor receptor 2	813.1860577	0.193619621	451.5885556	0.235326753	**1.800723352**	**0.01626331**
Fgfr1	fibroblast growth factor receptor 1	300.4716334	0.813353765	255.3859332	0.794570092	1.176539482	0.179540765
Fgfr3	fibroblast growth factor receptor 3	140.6777924	0.565431926	188.2482391	0.813949118	-1.338151785	1
Fgfr4	fibroblast growth factor receptor 4	97.98335351	0.336423871	103.2283889	0.225590878	-1.053529862	0.145817534

doi:10.1371/journal.pone.0087038.t002

Table 3. Expression of Genes in the EGF pathways

		LE		IE		LE/IE	
symbol	name	ave.int	p-val	ave.int	p-val	fold	p.val
The EGF family							
Ligands							
Areg	amphiregulin	155.3082961	0.133546244	196.8743744	0.233004491	-1.267635917	0.478968664
Hbegf	heparin-binding EGF-like growth factor	128.9845997	0.297282478	167.4743744	0.384089575	-1.298405971	0.478845479
Tgfa	transforming growth factor alpha	105.2105058	0.589279991	153.7290675	0.484086582	-1.461157005	0.202676617
Nrg1	neuregulin 1	98.00624272	0.715140496	155.8413258	0.467264689	-1.590116318	0.685383852
Btc	betacellulin, epidermal growth factor family member	87.55213556	0.930827589	117.8289953	0.865162398	-1.345815205	0.715209746
Nrg2	neuregulin 2	83.82453012	0.983653113	79.467853	0.538534554	1.054823139	NA
Nrg3	neuregulin 3	58.13060811	0.355939687	103.0507744	0.922549334	-1.772745509	0.478847044
Ereg	epiregulin	52.18751712	0.234405883	55.55150234	0.184028108	-1.064459576	0.565380436
Egf	epidermal growth factor	47.88076511	0.161070096	48.01846247	0.105485701	-1.002875839	0.478845479
Receptors							
Erbb2	v-erb-b2 erythroblastic leukemia viral oncogene homolog 2	400.0763611	0.357543272	224.2186429	0.920362594	**1.784313543**	**0.018738394**
Egfr	epidermal growth factor receptor	268.515161	0.647969842	410.0439401	0.18271137	-1.527079285	0.478850402
Erbb3	v-erb-b2 erythroblastic leukemia viral oncogene homolog 3	184.0990756	0.985729198	174.7380987	0.682470129	1.05357147	0.273357054
Erbb4	v-erb-a erythroblastic leukemia viral oncogene homolog 4	54.61474781	0.163158368	129.3400888	0.30614936	-2.368226422	0.472018438

doi:10.1371/journal.pone.0087038.t003

been fully understood. Genetic knockout studies in mice have helped to elucidate the roles of some of the signaling molecules. Using this approach, it is shown that multiple EGFR ligands act additively to regulate eyelid morphogenesis. Thus, whereas the *Hb-egf*-null and *Tgfα*-null mice display occasionally "open-eye" phenotype, the compound mutants, i.e. *Hb-egf(−/−)Tgfα(+/−)* and *Hb-egf(+/−)Tgfα(−/−)*, have a slightly increased penetrance, and the double homozygous null mice have a drastically increased penetrance of the phenotype. Furthermore, the triple null mice, lacking three of the EGFR ligand genes, *Egf*, *Areg* and *Tgfα*, exhibit a severe "eye-open" phenotype [37]. Similarly, by generating a series of genetic mutant strains, Huang, *et. al.* have shown the BMP signaling is specifically involved in eyelid closure. Mice lacking components of the TGFβ pathways have normal eyelid development, but those with impaired BMP signaling display an 'eyelid open at birth' phenotype [13].

The most remarkable feature of lid closure is the shape change and migration underwent by the epithelial cells at the "tip" of the eyelid. This is accompanied by activation of specific morphogenetic pathways. It is possible that the tip cells have unique surrounding tissues, i.e., microenvironments, which produce morphogens for specific activation of signaling pathways. Alternatively, the tip cells may have unique gene expression thereby acquiring new signaling and morphogenetic properties. Gene expression is a crucial facet of its function, and many genes essential for eyelid closure, such as *Tgfα*, *Hb-egf*, *Activinβb* and *Map3k1*, are indeed up-regulated in the developing eyelid epithelium [6,20,38,39].

In the present work, we applied a global approach to compare gene expression profiles in epithelial cells isolated from the tip (leading edge, LE) and the inner surface (inner epithelium, IE) of the embryonic eyelid. We evaluated the relative abundance in expression of genes whose products might constitute the major "eyelid closure pathways". Results may help to understand how signals are distinctly regulated in the LE cells and provide guidance for selecting "genes of interest" for expression and knockout studies.

Materials and Methods

Experimental animals

C57BL/6 fetuses were collected at E15.5. Euthanasia of the E15.5 fetuses was done by decapitation with surgical scissors, and genotypes were determined by PCR. Experiments conducted with these animals were carried out in strict accordance with the recommendations in the Guide for the Care and Use of Laboratory Animals of the National Institutes of Health. The protocol was approved by the Committee on the Ethics of Animal Experiments of the University of Cincinnati (Protocol no. 06-04-19-01).

Tissue and cell preparation, RNA and cDNA generation and microarray

This process was done as previously described [40]. Briefly, the heads of E15.5 fetuses were embedded in Tissue-Tek OCT medium (Sakura Finetek USA) and stored in −80°C. Eight μm coronal sections were mounted on plain uncoated glass slides, dehydrated and stained with HistoGene LCM frozen section staining kit, and were used for LCM following the manufacturer's protocol (Molecular Devices). Cells from 4 sections were collected

Table 4. Expression of genes in the *Lgr* and *Gpr* families

		LE		IE		LE/IE	
symbol	**name**	**ave.int**	**p-val**	**ave.int**	**p-val**	**fold**	**p.val**
Lgr							
Lgr4	leucine-rich repeat-containing G protein-coupled receptor 4	157.3388508	0.404500028	383.3124767	0.25234085	-2.43622268	0.287853304
Lgr6	leucine-rich repeat-containing G protein-coupled receptor 6	116.419403	0.783191878	103.8732732	0.481567664	1.120783041	0.129157861
Lgr5	leucine rich repeat containing G protein coupled receptor 5	55.18917435	0.267528025	125.0686009	0.659286312	-2.266179959	0.596789619
Gpr							
Gpr125	G protein-coupled receptor 125	220.1038045	0.021084389	289.8375491	0.026009754	-1.316822078	0.500824711
Gpr56	G protein-coupled receptor 56	218.8178318	0.021853992	171.4743744	0.303240853	1.2760964	0.01999301
Gpr20	G protein-coupled receptor 20	211.4585922	0.026852976	316.8945328	0.01511878	-1.498612705	0.839414104
Gpr35	G protein-coupled receptor 35	180.0479953	0.065600296	211.299815	0.132169905	-1.173574938	0.746554847
Gpr180	G protein-coupled receptor 180	175.9631725	0.073778453	225.2654962	0.098636269	-1.280185467	0.478842536
Gpr89	G protein-coupled receptor 89	175.0870638	0.075663315	259.1367522	0.04874379	-1.480045108	0.860737542
Gpr3	G-protein coupled receptor 3	166.2545002	0.097617959	256.2424001	0.051748411	-1.541265949	0.33371539
Gpr27	G protein-coupled receptor 27	164.4406301	0.102869023	147.2047335	0.495484149	1.117087924	0.000579647
Gpr107	G protein-coupled receptor 107	162.419388	0.109055871	229.0743744	0.09108073	-1.410388114	0.137248811
Gpr108	G protein-coupled receptor 108	145.2163784	0.17923789	191.0189953	0.202107027	-1.315409442	0.911106857
Gpr137	G protein-coupled receptor 137	127.2392185	0.299750484	136.5343716	0.61000012	-1.073052579	0.203778073
Gpr135	G protein-coupled receptor 135	124.301855	0.325673932	117.9937349	0.859217628	1.053461483	0.370495905
Gpr119	G-protein coupled receptor 119	123.7604085	0.330676321	130.9329503	0.678452003	-1.057955059	0.157171461
Gpr75	G protein-coupled receptor 75	123.6542976	0.331665052	135.7166762	0.619626637	-1.097549207	0.216351769
Gpr44	G protein-coupled receptor 44	123.3665465	0.334360194	130.317495	0.686333622	-1.056343868	0.496977287
Gpr124	G protein-coupled receptor 124	115.0903184	0.42110489	149.9910593	0.468845533	-1.303246541	0.478842349
Gpr39	G protein-coupled receptor 39	97.00347273	0.682938697	105.2282022	0.933334644	-1.08478799	0.33371539
Gpr123	G protein-coupled receptor 123	96.88645603	0.684992273	125.8634937	0.745514901	-1.29908244	0.247272771
Gpr85	G protein-coupled receptor 85	96.61297529	0.689810486	139.7885876	0.572910687	-1.446892481	0.674432534
Gpr30	G protein-coupled receptor 30	96.58976307	0.690220652	107.3732646	0.969969091	-1.111642281	0.186297098
Gpr153	G protein-coupled receptor 153	94.94188296	0.719823958	98.13033433	0.808122405	-1.033583191	0.312765421
Gpr137b-ps	G protein-coupled receptor 137B, pseudogene	94.78743922	0.722647465	282.2968287	0.030313391	-2.978209255	0.680474406
Gpr81	G protein-coupled receptor 81	92.51193082	0.765219363	123.7269258	0.775238854	-1.337415884	0.469995365
Gpr4	G protein-coupled receptor 4	92.03372555	0.774396617	103.5068225	0.903492859	-1.124661877	0.85686891
Gpr179	G protein-coupled receptor 179	91.13654808	0.791829182	100.0755366	0.842964993	-1.098083466	0.327688347
Gpr97	G protein-coupled receptor 97	90.49460245	0.804473656	96.21870568	0.773579498	-1.063253532	0.341054528
Gpr172b	G protein-coupled receptor 172B	88.72249257	0.8401129	97.276255	0.792722632	-1.096410303	0.037918301
Gpr171	G protein-coupled receptor 171	85.5606136	0.906315064	191.2743744	0.201031884	-2.235542341	0.288166398
Gpr25	G protein-coupled receptor 25	84.40014173	0.931423514	98.44886788	0.813850833	-1.166453822	0.065281383
Gpr6	G protein-coupled receptor 6	82.59264406	0.971357511	74.27593798	0.380077813	1.111970395	0.815470951
Gpr137b	G protein-coupled receptor 137B	81.25127761	0.998384708	107.3979928	0.970387644	-1.321800665	0.713122571
Gpr114	G protein-coupled receptor 114	80.90069545	0.990392729	82.19300262	0.517720661	-1.015973993	0.496210735
Gpr17	G protein-coupled receptor 17	80.64630589	0.984572436	96.65240053	0.781439379	-1.198472757	0.48758246
Gpr173	G-protein coupled receptor 173	80.57298468	0.982891617	102.3705866	0.883595209	-1.270532387	0.865882429
Gpr83	G protein-coupled receptor 83	77.34451159	0.907515055	118.4744165	0.851944372	-1.531775352	0.664800049
Gpr183	G protein-coupled receptor 183	75.90513232	0.873125838	136.6792593	0.608307331	-1.800658995	0.977344711
Gpr133	G protein-coupled receptor 133	73.77656211	0.821530114	92.57027338	0.707052638	-1.254738236	0.310248937
Gpr126	G protein-coupled receptor 126	72.44315307	0.788832074	232.0775545	0.085538588	-3.203581631	0.138923358
Gpr18	G protein-coupled receptor 18	72.21733384	0.783270351	182.9476886	0.239134407	-2.533293309	0.501943232
Gpr84	G protein-coupled receptor 84	72.20812693	0.783043458	86.08696737	0.588271302	-1.192206072	0.224588613

Table 4. Cont.

		LE		IE		LE/IE	
symbol	**name**	**ave.int**	**p-val**	**ave.int**	**p-val**	**fold**	**p.val**
Gpr37l1	G protein-coupled receptor 37-like 1	72.13222905	0.781172645	98.78720469	0.819925994	-1.369529349	0.431585749
Gpr144	G protein-coupled receptor 144	72.06972089	0.779631349	79.31147279	0.466480372	-1.100482586	0.132102738
Gpr157	G protein-coupled receptor 157	71.40005822	0.763090782	96.67623462	0.781870956	-1.354007784	0.358178624
Gpr156	G protein-coupled receptor 156	70.40086729	0.738326035	68.5804486	0.289316439	1.026544281	0.478847201
Gpr146	G protein-coupled receptor 146	69.62364684	0.719006489	53.54305799	0.104400524	1.300330042	0.13090816
Gpr160	G protein-coupled receptor 160	69.39114229	0.713219524	74.72537227	0.387587547	-1.076871915	0.337863882
Gpr77	G protein-coupled receptor 77	69.38658457	0.713106053	64.65720239	0.232512432	1.073145481	0.246294322
Gpr68	G protein-coupled receptor 68	65.98359522	0.628259898	89.82589824	0.656736889	-1.361336828	0.836126668
Gpr162	G protein-coupled receptor 162	63.89859714	0.576464248	71.74780097	0.338720298	-1.122838437	0.753129884
Gpr132	G protein-coupled receptor 132	61.01745433	0.505773427	65.42941991	0.243272256	-1.072306615	0.770153611
Gpr111	G protein-coupled receptor 111	60.35405182	0.489718441	54.49499311	0.113259572	1.107515542	0.379862366
Gpr62	G protein-coupled receptor 62	58.81170703	0.45281891	71.99871533	0.342753671	-1.224224206	0.438288689
Gpr26	G protein-coupled receptor 26	58.61960404	0.448269774	80.90301094	0.494654237	-1.380135746	0.470158493
Gpr15	G protein-coupled receptor 15	57.40978461	0.419890293	57.81324406	0.147347983	-1.007027712	0.153990594
Gpr161	G protein-coupled receptor 161	55.91072381	0.385447822	107.498657	0.972090592	-1.922684052	0.512145141
Gpr45	G protein-coupled receptor 45	55.40839734	0.374105939	53.82411607	0.106973001	1.029434413	0.140431857
Gpr151	G protein-coupled receptor 151	54.78053147	0.360082493	85.45866943	0.576815937	-1.560018991	1
Gpr65	G-protein coupled receptor 65	54.05701451	0.344145124	146.8162858	0.499301801	-2.715952538	0.158633441
Gpr182	G protein-coupled receptor 182	53.23426477	0.326329103	85.11797113	0.57061356	-1.598932032	0.567583183
Gpr139	G protein-coupled receptor 139	53.02682408	0.321891129	92.38956386	0.703743558	-1.742317506	0.258601234
Gpr21	G protein-coupled receptor 21	52.0328213	0.300942497	72.73913052	0.354750161	-1.397947078	0.741406994
Gpr158	G protein-coupled receptor 158	51.92947168	0.29879543	63.41336159	0.215644175	-1.221143977	0.637090301
Gpr63	G protein-coupled receptor 63	50.9959338	0.279678293	97.86797672	0.803397981	-1.919132947	0.946152571
Gpr155	G protein-coupled receptor 155	49.97110494	0.259290745	92.12694599	0.698933085	-1.843604341	0.324933584
Gpr176	G protein-coupled receptor 176	48.96242303	0.239872194	53.89486012	0.107626211	-1.100739236	0.212932186
Gpr19	G protein-coupled receptor 19	48.77902167	0.236413235	88.48209068	0.632092019	-1.813937378	0.478842035
Gpr116	G protein-coupled receptor 116	47.64519495	0.215538201	95.65763979	0.763393274	-2.007708015	0.237971027
Gpr37	G protein-coupled receptor 37	46.63567635	0.197714832	78.6480309	0.45484197	-1.686434873	0.33350725
Gpr12	G-protein coupled receptor 12	43.87164829	0.152825917	89.07378877	0.642941053	-2.030326925	0.25456221
Gpr61	G protein-coupled receptor 61	38.39824197	0.082156744	90.09705371	0.661711292	-2.346384863	0.725656569
Gpr137c	G protein-coupled receptor 137C	38.28835404	0.080994315	89.45583486	0.649948364	-2.33637191	NA

doi:10.1371/journal.pone.0087038.t004

on one LCM cap and lysed for RNA harvesting. The lysates from each fetus were pooled and processed as one biological sample. It was estimated that 10 ng and 15 ng total RNA were obtained from LE and IE eyelid epithelium, respectively, per fetus.

RNA was analyzed by Agilent 2100 Bioanalyzer (Agilent, Santa Clara, CA) and samples with RNA Integrity Number (RIN) >5.5 were processed for cDNA amplification. cDNA amplification and biotinylation was done using Ovation Pico WTA System (NuGEN, San Carlos, CA) following the manufacturer's instructions. Specifically, RNA (10 ng) was processed into first strand cDNA, a DNA/RNA heteroduplex, and thereafter a linear isothermal amplified cDNA. The amplified cDNA was purified with a PCR Purification Kit (QIAGEN, Valencia, CA).

The cDNAs from each fetus were considered one biological sample and 3 samples were used for triplicate hybridization on the Affymetrix GeneChip Mouse Gene 1.0 ST array (P/N 901168, Affymetrix, Santa Clara, CA). The arrays were hybridized with 15 μg of fragmented aRNA. The hybridization, staining, and washing are carried out using the Affymetrix GeneChip Hybridization Wash and Stain Kit (P/N 900720) following the manufacturer's protocols. The arrays were hybridized for 16 hr at 45°C using Affymetrix Hybridization Oven 640 (P/N 800139). FS450-0001 protocol was used for staining and washing the GeneChips using the Affymetrix Fluidics Station 450 (P/N 00-0079). The GeneChips were scanned with Affymetrix GeneChip Scanner 3000 7G Plus using Affymetrix GeneChip Command Console 3.2.3.1515 software and Affymetrix preset settings.

Quantitative RT-PCR

Quantitative PCR was performed using an MX3000p thermal cycler system and SYBR Green QPCR Master Mix (Stratagene), using conditions optimized for each target gene primers with efficiency greater than 85%, cycles less than 29 and sample locations on the plates been randomized. The PCR products were subjected to melting curve analysis and the relative cycle differences in qRT-PCR were determined using ΔCt, as described

Table 5. Expression of genes in the Adams family

		LE		IE		LE/IE	
symbol	**name**	**ave.int**	**p-val**	**ave.int**	**p-val**	**fold**	**p.val**
Adams							
Adam10	a disintegrin and metallopeptidase domain 10	**361.9310254**	**0.002605289**	**572.1144261**	**0.002197908**	-1.580727779	0.550173668
Adamtsl4	ADAMTS-like 4	186.7402441	0.118746409	183.2381962	0.566007252	1.019111997	0.211012267
Adam17	a disintegrin and metallopeptidase domain 17	179.240216	0.14151102	327.0666618	0.065754322	-1.824739275	0.43979387
Adam15	a disintegrin and metallopeptidase domain 15	176.91194	0.149437176	236.3028883	0.258585267	-1.335709101	0.86373439
Adamts17	a disintegrin-like and metallopeptidase with thrombospondin type 1, 17	166.285723	0.191649211	155.1157197	0.83380408	1.072010776	0.17838096
Adam33	a disintegrin and metallopeptidase domain 33	143.2533418	0.327655809	187.3018386	0.534022951	-1.307486696	0.607122322
Adamts10	a disintegrin-like and metallopeptidase with thrombospondin type 1, 10	135.1273739	0.394870436	188.5363387	0.524624481	-1.39524904	0.323396275
Adam1a	a disintegrin and metallopeptidase domain 1a	125.7803888	0.487891176	142.3710583	0.982078417	-1.131901878	0.302441913
Adamtsl5	ADAMTS-like 5	118.8409891	0.569188872	156.684171	0.816684342	-1.318435434	0.219403185
Adamts2	a disintegrin-like and metallopeptidase with thrombospondin type 1, 2	114.1361944	0.630738755	178.4675506	0.605650924	-1.563636772	0.981455083
Adamts1	a disintegrin-like and metallopeptidase with thrombospondin type 1, 1	109.4934689	0.696800634	288.2065321	0.117893987	-2.632180121	0.032615535
Adamts8	a disintegrin-like and metallopeptidase with thrombospondin type 1, 8	108.1270441	0.717269221	137.1852326	0.953251485	-1.268741171	0.670359886
Adamts7	a disintegrin-like and metallopeptidase with thrombospondin type 1, 7	104.7353254	0.770104259	126.3711396	0.811832594	-1.206576091	0.419966026
Adamts12	a disintegrin-like and metallopeptidase with thrombospondin type 1, 12	103.266259	0.793884786	253.7738818	0.198575014	-2.457471436	0.15311868
Adam4	a disintegrin and metallopeptidase domain 4	101.4912963	0.823334302	103.9723183	0.506418509	-1.024445663	0.359728774
Adam11	a disintegrin and metallopeptidase domain 11	96.48278062	0.910581493	93.32233476	0.367807843	1.033865911	0.16144701
Adam9	a disintegrin and metallopeptidase domain 9	92.75365702	0.979347597	188.8591255	0.522191173	-2.036136705	0.321859941
Adamtsl2	ADAMTS-like 2	90.38008471	0.975311941	104.9617327	0.519752615	-1.161336959	0.15311868
Adamtsl1	ADAMTS-like 1	89.39194852	0.956099857	117.7630678	0.694883169	-1.317378911	0.689678828
Adam19	a disintegrin and metallopeptidase domain 19	89.37741331	0.955815834	139.0754455	0.977089116	-1.556046884	0.632565024
Adamts16	a disintegrin-like and metallopeptidase with thrombospondin type 1, 16	89.1800757	0.951955786	99.78955189	0.450753967	-1.118966889	0.59922473
Adam22	a disintegrin and metallopeptidase domain 22	88.31886637	0.935023936	180.7780221	0.586164894	-2.046878878	0.359894666
Adam8	a disintegrin and metallopeptidase domain 8	86.51484226	0.899121169	92.0647805	0.35224885	-1.064150128	0.27105888
Adamts13	a disintegrin-like and metallopeptidase with thrombospondin type 1, 13	85.83956723	0.885539162	88.47392725	0.309067767	-1.030689344	0.478844207
Adamts9	a disintegrin-like and metallopeptidase with thrombospondin type 1, 9	83.27099934	0.833234446	189.3210225	0.518726499	-2.273552906	0.254563761
Adamts18	a disintegrin-like and metallopeptidase with thrombospondin type 1, 18	81.4196745	0.794981469	168.7064225	0.694045146	-2.072059653	0.162103461
Adamts14	a disintegrin-like and metallopeptidase with thrombospondin type 1, 14	80.27793265	0.771197631	82.77491987	0.244956077	-1.031104279	0.439155995
Adamts19	a disintegrin-like and metallopeptidase with thrombospondin type 1, 19	69.27461445	0.539213852	109.3590982	0.579553669	-1.578631639	0.390223674
Adamts4	a disintegrin-like and metallopeptidase with thrombospondin type 1, 4	68.27128822	0.518287473	74.72450982	0.165658834	-1.094523214	0.478842805
Adam21	a disintegrin and metallopeptidase domain 21	60.66601728	0.36550739	64.64919733	0.088605328	-1.065657517	0.999197582

Table 5. Cont.

		LE		IE		LE/IE	
symbol	**name**	**ave.int**	**p-val**	**ave.int**	**p-val**	**fold**	**p.val**
Adamts20	a disintegrin-like and metallopeptidase with thrombospondin type 1, 20	58.83741845	0.331040492	97.20251711	0.417043299	-1.652052719	0.478849238
Adam12	a disintegrin and metallopeptidase domain 12	55.75657162	0.275742738	151.6194647	0.872877811	-2.719311111	0.196227734
Adamts5	a disintegrin-like and metallopeptidase with thrombospondin type 1, 5	55.55758605	0.272304468	141.9022559	0.987828457	-2.554147254	0.09184658
Adamts3	a disintegrin-like and metallopeptidase with thrombospondin type 1, 3	51.72989842	0.209742874	170.6776655	0.675392791	-3.299400748	0.478860496
Adamts15	a disintegrin-like and metallopeptidase with thrombospondin type 1, 15	51.52479453	0.206595412	79.74566033	0.213438929	-1.547714281	0.219403185
Adamtsl3	ADAMTS-like 3	47.33432389	0.147349513	66.40359283	0.10011701	-1.402863448	0.67686266
Adam23	a disintegrin and metallopeptidase domain 23	43.57759051	0.103048326	117.4744258	0.69092512	-2.695753125	0.127323609
Adamts6	a disintegrin-like and metallopeptidase with thrombospondin type 1, 6	40.47668384	0.073119037	142.2520509	0.983536216	-3.514419598	0.153396483

doi:10.1371/journal.pone.0087038.t005

[41]. The ΔCt value for each sample was determined using the cycle threshold (Ct) value of the specific gene normalized to that of *Gapdh*. The fold change was calculated based on the ratio between LE versus IE (control) samples, designated as 1. Data are based on triplicate reactions of at least 3 biological samples.

Statistical and bioinformatics analyses

Array data (GEO repository, accession no. GSE39240) were analyzed at gene level using statistical software R and the limma package of Bioconductor [42] with custom CDF downloaded from BrainArray [43]. Data pre-processing, including background correction and normalization, was performed using RMA. Array quality was assessed using the Array Quality Metrics package of Bioconductor [44]. Statistical significance of differential gene expression between LE and IE samples were established based on empirical Bayes linear model as implemented in limma package [42].

Functional enrichment analysis of differentially expressed genes was performed using the logistic regression based LRpath methodology [45] as implemented in the R package CLEAN [46]. The gene list used in the functional enrichment analysis came from genes associated with Gene Ontology terms [47]. The statistical significance of gene list enrichment was determined based on the False Discovery Rate (fdr) cut-off of 0.1. The statistical significance of deviations of average gene expression levels for genes within the same group were established by calculating gene specific z-statistics and comparing it to the standard Normal distribution. The z-statistic was calculated by subtracting the average of expression levels of all genes in the group from the expression level of the gene and dividing the difference by the standard deviation of the expression levels within the group.

Results and Discussion

Gene expression profiles in the developing eyelid epithelium

To identify the molecular signatures of eyelid closure, we collected mouse fetuses at E15.5, a developmental stage immediately before the eyelid beginning to close. We used laser capture microdissection (LCM) to isolate epithelial cells from the leading edge (LE) and inner surface epithelium (IE). The samples were used for expression array and gene expression signatures were analyzed as described [40].

To determine whether the LE and IE cells were different at E15.5, we analyzed the expression data by Gene Ontology (GO). The LE cells were enriched for genes involved in epidermis development, transcription factor activity, pattern specification and odontogenesis. By contrast, the IE cells were enriched for genes for muscle development, RNA splicing, microtubule organization and centrosomes (Table 1). The GO signatures suggest that the E15.5 LE and IE cells have already departed to distinct paths from their common origin - the ocular surface ectoderm.

Expression of signaling molecules in the FGF and EGF pathways

To evaluate whether the LE and IE cells had differential expression of signaling molecules, we examined genes involved in the FGF and EGF pathways, known to be involved in eyelid closure. The fibroblast growth factor (FGF) family has 22 ligands and four membrane-bound receptors, FGFR 1-4, with different ligand binding affinities [48,49]. In LE and IE cells, the *Fgfr2* was the most abundantly expressed receptor gene, and *Fgf9* was the highly expressed ligand gene (Table 2). Between LE and IE, there was no major difference in the expression of genes belonging to the families of FGF ligands and receptors, except for *Fgfr2* (Table 2). The level of *Fgfr2* was 1.8-fold higher in LE cells, suggesting that the LE cells might be more responsive to FGF signals than the IE cells.

Previously, we have shown that FGF9 expression was decreased in LE cells of *Map3k1* knockout fetuses corresponding to failure of eyelid closure [40]. FGF9 could act in an autocrine fashion to induce epithelial branching, or it could send signals to the mesenchyme to induce PITX2 and FGF10. FGF10 in turn could trans-activate FGFR in epithelial cells and stimulate epithelial budding [50,51]. Genetic studies show that FGF10 is crucial for eyelid closure, but FGF9, though required for sex determination and reproductive system development, lung embryogenesis, and inner ear morphogenesis, is dispensable for eyelid development

Table 6. Expression of genes in the TGFβ pathways

		LE		IE		LE/IE	
symbol	**name**	**ave.int**	**p-val**	**ave.int**	**p-val**	**fold**	**p.val**
The TGFβ family							
Ligands							
Bmp7	bone morphogenetic protein 7	273.8032153	0.067190002	164.4743744	0.782003153	1.664716564	0.108606617
Inhbb	inhibin beta-B	189.8249605	0.267867653	229.6743744	0.349920499	-1.209927155	0.015593156
Bmp4	bone morphogenetic protein 4	187.94911	0.276418245	187.8661392	0.590049741	1.000441648	0.143749699
Gdf10	growth differentiation factor 10	183.9074068	0.295778825	359.5450161	0.069068988	-1.95503282	0.661905204
Bmp2	bone morphogenetic protein 2	182.4613117	0.303028915	135.916909	0.921038359	1.342447478	0.212844348
Bmp1	bone morphogenetic protein 1	177.4112267	0.329755901	223.090068	0.380257649	-1.257474356	0.254597392
Tgfb2	transforming growth factor, beta 2	172.6298162	0.35719415	300.8077524	0.142523738	-1.742501724	0.329864054
Bmp8a	bone morphogenetic protein 8a	172.1103393	0.360306504	164.7585892	0.779391571	1.044621346	0.089033623
Gdf11	growth differentiation factor 11	159.4675951	0.44467919	175.0468033	0.689538262	-1.097695135	0.201245908
Bmp3	bone morphogenetic protein 3	148.1166656	0.536120106	202.4442107	0.492685372	-1.366788875	0.477486266
Gdf7	growth differentiation factor 7	147.8721307	0.538269393	153.7647042	0.8854851	-1.039849115	0.156938123
Inhba	inhibin beta-A	130.5738373	0.711324184	197.0395548	0.52691848	-1.509027833	0.712026446
Inha	inhibin alpha	130.1272773	0.716364388	204.5980265	0.479628814	-1.572291611	0.237387534
Bmp6	bone morphogenetic protein 6	125.274918	0.773059365	146.8885336	0.957046207	-1.172529473	0.286103958
Nodal	nodal	103.8101562	0.934420257	85.88759992	0.315528911	1.208674551	0.247190059
Nog	noggin	100.0350956	0.876554259	83.19324041	0.286197111	1.202442592	0.195250499
Tgfb1	transforming growth factor, beta 1	82.15218608	0.586613596	155.2142228	0.87090424	-1.889349879	0.210538535
Bmp8b	bone morphogenetic protein 8b	81.76056963	0.580144573	102.4426736	0.511615715	-1.252959391	0.578881901
Inhbc	inhibin beta-C	74.08385854	0.454687654	82.33694939	0.277085231	-1.111402011	0.542313176
Inhbe	inhibin beta E	69.57742791	0.383541072	74.89766277	0.202836798	-1.076464955	0.479105423
Tgfb3	transforming growth factor, beta 3	66.35517701	0.334591515	165.0505869	0.776715748	-2.487380704	0.254565854
Gdf9	growth differentiation factor 9	64.46053434	0.306763225	71.94859953	0.176159291	-1.116165112	0.164059633
Gdf6	growth differentiation factor 6	56.98847182	0.205865955	140.1852498	0.969536519	-2.459887856	0.274524202
Gdf3	growth differentiation factor 3	55.99339008	0.193684893	108.15508	0.582739207	-1.931568705	0.511633304
Gdf5	growth differentiation factor 5	51.66075472	0.14467988	60.11493281	0.087859418	-1.163647979	0.478845373
Bmp5	bone morphogenetic protein 5	51.55346944	0.143554136	314.8319068	0.11964688	-6.106900471	0.022920742
Gdf2	growth differentiation factor 2	50.43190792	0.132051407	52.21430519	0.047202918	-1.03534265	0.201766807
receptor							
Acvr2a	activin receptor IIA	**785.286694**	**0.006949311**	824.9994488	0.053983644	-1.050571027	0.535202305
Bmpr2	bone morphogenic protein receptor, type II	407.8628762	0.093450343	551.8506099	0.175491837	-1.353029761	0.371468892
Bmpr1a	bone morphogenetic protein receptor, type 1A	198.0829607	0.581647187	565.1672519	0.164924701	-2.853184594	0.028854135
Crim1	cysteine rich transmembrane BMP regulator 1	153.691022	0.876649887	204.0309462	0.951248863	-1.327539784	0.582802236
Tgfbr3	transforming growth factor, beta receptor III	143.0723153	0.965261747	200.257104	0.930110624	-1.399691503	0.323764976
Bambi	BMP and activin membrane-bound inhibitor, homolog	135.4573152	0.96669452	189.5920525	0.868484804	-1.399644251	1
Tgfbr1	transforming growth factor, beta receptor I	122.9008043	0.846582157	462.154534	0.27030705	-3.760386569	0.147558346
Acvrl1	activin A receptor, type II-like 1	116.9128312	0.786093483	136.2815587	0.525171941	-1.165668107	0.633311024
Tgfbr2	transforming growth factor, beta receptor II	112.9823508	0.745389803	163.7414235	0.70827237	-1.449265503	0.319010671
Acvr1b	activin A receptor, type 1B	101.4320918	0.622064638	110.4656142	0.350173625	-1.089059806	0.526331743
Acvr1	activin A receptor, type 1	100.3229914	0.609999096	247.9101709	0.82894344	-2.471120203	0.016173055
Acvr2b	activin receptor IIB	100.265421	0.609372034	111.8813641	0.359598279	-1.115851935	0.180539507
Bambi-ps1	BMP and activin membrane-bound inhibitor, pseudogene	80.5511445	0.393972944	80.94115829	0.168579167	-1.004841816	0.358188963

Table 6. Cont.

		LE		IE		LE/IE	
symbol	**name**	**ave.int**	**p-val**	**ave.int**	**p-val**	**fold**	**p.val**
Bmpr1b	bone morphogenetic protein receptor, type 1B	76.22336452	0.347952441	116.7512861	0.392273989	-1.531699457	0.792545942
Tgfbrap1	transforming growth factor, beta receptor associated protein 1	73.74312689	0.32209407	141.4743747	0.560446165	-1.918475398	0.475558452
intracellular							
Smad2	MAD homolog 2 (Drosophila)	629.9527764	0.095677501	818.2805642	0.092838612	-1.298955406	0.195409967
Smad4	MAD homolog 4 (Drosophila)	354.4708292	0.364213634	447.8759579	0.391619063	-1.263505826	0.744635668
Smad3	MAD homolog 3 (Drosophila)	225.6921006	0.755336708	228.0715789	0.947457399	-1.010543029	0.158708217
Smad5	MAD homolog 5 (Drosophila)	219.8816039	0.781633462	368.1947529	0.555950137	-1.674513676	0.540729299
Smad1	MAD homolog 1 (Drosophila)	145.1756563	0.786661254	192.0409924	0.763436753	-1.322818145	0.39420827
Smad6	MAD homolog 6 (Drosophila)	110.418776	0.527526974	169.8452718	0.639157382	-1.538191944	0.835712394
Smad7	MAD homolog 7 (Drosophila)	96.23172938	0.41606715	127.125665	0.387073288	-1.321036895	0.180320764
Crim1	MAD homolog 9 (Drosophila)	59.54834067	0.147995136	84.36472138	0.154019199	-1.416743446	0.243731275

doi:10.1371/journal.pone.0087038.t006

[52–54]. Since FGF10 was almost undetectable in LE and IE cells, it is possible that this ligand is produced by the underlying mesenchymal cells, responsible for activation of FGFR2 in the eyelid epithelium [5,6].

The epidermal growth factor (EGF) pathway operates in an autocrine fashion, such that ligands produced by the epithelial cells can activate receptors on the same or nearby cells [6,38,55,56]. The mammalian system has nine ligands, which are first expressed as transmembrane proteins comprising a signal sequence, a transmembrane domain and the EGF domain(s). The ligands are then activated by ectodomain shedding that releases the EGF domain from the membrane-bound precursors. This is carried out by members of disintegrin and metalloproteases (ADAMS) family of type I transmembrane Zn-dependent proteases. There are four EGF receptor tyrosine kinases, including EGFR/ERBB1, ERBB2, ERBB3 and ERBB4 [57]. Activation of the receptors is also facilitated by members of the leucine-rich repeat containing G-protein coupled receptor (LGR) and G protein-coupled receptor (GPCR) families.

In LE and IE cells, the *Egfr* and *Erbb2*, and several genes in the GPCR families, such as *Lgr4*, *Gpr125*, *Gpr20, Gpr180*, *Gpr89* and *Gpr3*, were abundantly expressed (Tables 3 and 4). Expression of *Adams10* was also abundant (Table 5). Expression of *Gpr56* was relatively abundant in LE cells, whereas expression of *Adam 17*, *Lgr4*, *Gpr107* and *Gpr137b-ps* was more abundant in IE cells. Compared to the IE cells, the LE cells had significantly higher expression of *Erbb2* (1.8-fold) and *Gpr56* (1.3-fold), but less expression of *Adamts1* (-2.6-fold).

The ligands specific for ERBB2 are unknown, but ERBB2 can dimerize with EGFR. The heterodimers, similar to the EGFR homodimers, can be activated by amphiregulin (AREG), heparin-binding EGF-like growth factor (HB-EGF) and transforming growth factor α (TGFα) [58]. Activation of the EGFR signaling is essential for embryonic eyelid closure [59]. Based on the relative abundance of receptor gene expression, the EGFR/EGFR and EGFR/ERBB2 dimers are likely to form in the developing eyelid epithelium. Specifically, the EGFR/ERBB2 may be the dominant form in LE, whereas the EGFR/EGFR is likely to be the predominant form in IE cells.

ADAMS10 is important for the development of blood vessels and central nervous system, as well as in pathological conditions such as inflammation and cancer [60]. Recently, it was shown that ADAMS10 may be the sheddase of notch receptors, involved in the release of the extracellular domain and mediating skin development; however, its role in eyelid development has not been established. On the other hand, the *Adams17* knockout mice exhibit the open eye phenotype [61]. ADAMS17 is the major sheddase of TGFα, amphiregulin, HB-EGF and epiregulin, and is essential for activation of EGFR during development [62,63]. Of the *Lgr/Gpcr* families, only the *Lgr4 (−/−)* mice have defective keratinocyte motility and produce the EOB phenotype. The *Lgr4*, also known as *Gpr48*, was known to play a role in HB-EGF-induced EGFR activation [64,65]. The expression of *Adams17* and *Lgr4* was both relatively abundant in the IE cells (Tables 4 and 5).

The most surprising observation made by the RNA array was that expression of EGFR ligands was scarce in the LE and IE cells (Table 3). This was in clear contrast to previous findings made by *in situ* hybridization and immunohistochemistry, which showed that expression of TGFα and HB-EGF was up-regulated in a group cells located at the tip of the developing eyelid [6,38,66]. The discrepancy could be explained if induction of ligand is a temporal-spatial event, taking place in a small number of cells and in a narrow window during embryogenesis. Hence, either ligand up-regulation was insignificant at E15.5, or the expression signals were masked or under-represented in the collectives of the LCM captured cells, exemplifying the limitations of this approach.

Taken together, the gene expression data confirm that many genetically identified "eyelid closure" factors, such as FGFR, EGFR, ADAMS17 and LGR4, are also relatively abundant in the LE and/or IE cells, but some highly expressed genes, including *Fgf9* and *Adam10*, are not known to be involved in eyelid closure. In comparison to the IE cells, the LE cells have higher expression of *Fgfr2* and *Erbb2*, which may contribute to differential signaling responses of these cells.

Expression of genes involved in the TGFβ signaling

The TGFβ superfamily consists of more than 30 structurally related ligands. They belong to the Bone Morphogenetic Proteins (BMPs), TGFβs and Activin/Inhibin subfamilies [67]. These ligands act selectively on seven type I and five type II receptors, resulting in receptor dimerization and activation. The receptors in turn activate two sets of so called R-SMAD. SMAD 1, 5, and 8 are

Table 7. Expression of genes in the Wnt pathways

		LE		IE		LE/IE	
symbol	**name**	**ave.int**	**p-val**	**ave.int**	**p-val**	**fold**	**p.val**
Wnt							
Ligands							
Apcdd1	adenomatosis polyposis coli down-regulated 1	483.5614722	0.053814884	277.7634161	0.800811376	**603.839414**	**0.011267485**
Sfrp2	secreted frizzled-related protein 2	**348.8687731**	**0.020922218**	**654.0519384**	**0.037660546**	9263.508027	0.174835606
Sfrp4	secreted frizzled-related protein 4	249.649771	0.112795852	316.9220374	0.273063678	914.2547726	0.40043203
Sfrp1	secreted frizzled-related protein 1	211.7568665	0.218783911	573.2261883	0.057477828	3684.148697	0.273488221
Dkk1	dickkopf homolog 1 (Xenopus laevis)	198.204605	0.277148921	180.9890829	0.736604814	269.0786174	0.391951411
Dkk2	dickkopf homolog 2 (Xenopus laevis)	177.2474096	0.398062954	**721.2937998**	**0.027019747**	**6559.921251**	0.012726284
Wnt10a	wingless related MMTV integration site 10a	176.4076412	0.403821253	184.4279311	0.717444422	245.8833545	0.478844672
Wnt2b	wingless related MMTV integration site 2b	160.0394529	0.532467804	182.5437831	0.727876583	219.871688	0.926769779
Wnt5b	wingless-related MMTV integration site 5B	142.8377647	0.70517094	175.1915846	0.770130122	185.4722475	0.479705404
Wnt10b	wingless related MMTV integration site 10b	142.5633067	0.708262603	116.9518638	0.798107856	178.6266175	0.478844678
Wnt4	wingless-related MMTV integration site 4	139.5806594	0.742557274	137.7167967	0.9727424	143.4919043	0.374613153
Wnt6	wingless-related MMTV integration site 6	135.1613805	0.795715493	160.3732491	0.863152443	156.5903932	0.078390545
Wnt9b	wingless-type MMTV integration site 9B	133.6151939	0.814972582	132.0830361	0.927644338	144.0370932	0.289503817
Dkk3	dickkopf homolog 3 (Xenopus laevis)	110.7032791	0.86283769	136.6161576	0.964067385	114.8293998	0.206504995
Wnt7b	wingless-related MMTV integration site 7B	109.9061131	0.850570159	103.0750617	0.669327096	164.2038904	0.135756387
Wnt3a	wingless-related MMTV integration site 3A	105.5491979	0.782655232	115.4051747	0.784199907	134.5947595	0.279318999
Wnt9a	wingless-type MMTV integration site 9A	103.910602	0.756793175	95.49126948	0.595623787	174.45677	0.259209416
Wnt2	wingless-related MMTV integration site 2	91.74384223	0.562599042	83.13988271	0.472430417	194.1954603	0.625010844
Wnt8a	wingless-related MMTV integration site 8A	87.51527434	0.495855788	84.11155152	0.48219671	181.4928897	0.68835004
Wnt7a	wingless-related MMTV integration site 7A	84.77441059	0.453355276	82.50036825	0.466000878	181.9189931	0.203647077
Wnt11	wingless-related MMTV integration site 11	84.42137039	0.447937944	103.3922602	0.672364507	125.5589334	0.30355669
Dkkl1	dickkopf-like 1	80.6658968	0.391301917	49.5193887	0.155264947	**519.5370763**	**0.007020038**
Wnt5a	wingless-related MMTV integration site 5A	77.85246206	0.350290283	212.9173909	0.57775569	134.7497973	0.113472971
Wnt3	wingless-related MMTV integration site 3	70.09772231	0.245673781	64.97157496	0.292388531	239.7416961	0.080993879
Dkk4	dickkopf homolog 4 (Xenopus laevis)	61.9542671	0.153300371	67.89828852	0.32063799	193.2218548	0.228653762
Wnt16	wingless-related MMTV integration site 16	**47.68335129**	**0.046137884**	41.67678582	0.097927067	486.9271889	0.129518192
Receptors							
Fzd3	frizzled homolog 3 (Drosophila)	**621.1053146**	**0.041393074**	**813.2745816**	**0.010731489**	57876.90198	0.478857045
Fzd9	frizzled homolog 9 (Drosophila)	421.0632821	0.122596071	392.1751139	0.199012898	2115.758764	0.87130258
Dvl3	dishevelled 3, dsh homolog (Drosophila)	413.3018893	0.128448795	402.3131688	0.183945914	2246.866375	0.154874206
Lrp6	low density lipoprotein receptor-related protein 6	361.5150568	0.177156701	431.6042255	0.146840648	2461.954923	0.583273548
Lrpap1	low density lipoprotein receptor-related protein AP-1	251.7744179	0.374371039	394.0853272	0.196076999	1284.058914	0.305691833
Fzd6	frizzled homolog 6 (Drosophila)	228.5769945	0.444226001	253.913148	0.59664302	383.105118	0.809625026
Lrp1	low density lipoprotein receptor-related protein 1	203.9297815	0.535517337	263.3174719	0.553577155	368.3854721	0.263717473
Daam1	dishevelled associated activator of morphogenesis 1	180.844634	0.640904694	283.032779	0.472862601	382.4464733	0.627127554
Fzd7	frizzled homolog 7 (Drosophila)	160.7760067	0.751649955	186.5780299	0.995186416	161.5536588	0.434764207
Lrp4	low density lipoprotein receptor-related protein 4	150.3594548	0.817266008	180.2743744	0.947588434	158.6759076	0.546664989
Lrp12	low density lipoprotein-related protein 12	149.1675011	0.825158313	308.3467702	0.386144171	386.3000201	0.392040335
Fzd10	frizzled homolog 10 (Drosophila)	143.5471885	0.863477711	146.15934	0.667091155	215.1837683	0.093092703
Fzd5	frizzled homolog 5 (Drosophila)	133.4039545	0.937417185	179.4493072	0.941246041	141.731225	0.268788395
Lrp8	low density lipoprotein receptor-related protein 8	129.9627772	0.963950394	173.179921	0.892234598	145.6598718	0.96540813

Table 7. Cont.

		LE		IE		LE/IE	
symbol	**name**	**ave.int**	**p-val**	**ave.int**	**p-val**	**fold**	**p.val**
Daam2	dishevelled associated activator of morphogenesis 2	129.5253696	0.96737678	213.5127234	0.819485923	158.0568573	0.232134795
Lrp5	low density lipoprotein receptor-related protein 5	124.4582986	0.992036878	182.9363107	0.967875244	128.5891952	0.478848283
Fzd1	frizzled homolog 1 (Drosophila)	119.3852371	0.949735838	114.1795981	0.390301586	305.8794564	0.212940516
Dvl2	dishevelled 2, dsh homolog (Drosophila)	113.9854854	0.902859622	168.4318283	0.854195591	133.4419032	0.473187759
Fzd2	frizzled homolog 2 (Drosophila)	112.3533043	0.888313733	109.4746106	0.351250408	319.8666868	0.159410823
Lrp3	low density lipoprotein receptor-related protein 3	108.3015606	0.851451757	147.8738335	0.681889718	158.8256248	0.897879402
Dvl1	dishevelled, dsh homolog 1 (Drosophila)	107.1117074	0.84042385	145.3054246	0.659703892	**162.3633097**	**0.026996352**
Lrp10	low-density lipoprotein receptor-related protein 10	60.98575657	0.357857719	117.050989	0.414542002	147.1159889	0.47884479
Fzd8	frizzled homolog 8 (Drosophila)	55.12069055	0.294466513	85.06205341	0.170546176	323.2009761	0.478843194
Frzb	frizzled-related protein	52.66725106	0.26854277	167.7802652	0.848916887	62.04052699	0.356862886
Lrp11	low density lipoprotein receptor-related protein 11	44.59142388	0.18728742	85.39483827	0.172671979	258.2435451	0.202392746
Lrp2	low density lipoprotein receptor-related protein 2	40.27024362	0.147448705	95.17067762	0.239837412	167.9064298	0.254562864
Fzd4	frizzled homolog 4 (Drosophila)	31.47827903	0.07796015	128.7726731	0.515600438	61.05169179	0.187858824
Lrp2bp	Lrp2 binding protein	**26.76371598**	**0.04889444**	70.3777375	0.089199837	300.0422086	0.93675131
Intracellular destruction complex							
Ctnnb1	catenin (cadherin associated protein), beta 1	1048.175521	0.190192411	1125.036148	0.143218133	7318.734695	0.207958814
Gsk3b	glycogen synthase kinase 3 beta	676.0486341	0.434376095	825.1731378	0.278543966	2427.080521	0.920205733
Apc	adenomatosis polyposis coli	254.3465152	0.692184095	482.4879277	0.670699658	379.2256522	0.150092586
Gsk3a	glycogen synthase kinase 3 alpha	765.6427453	0.351520757	402.5362199	0.839207813	912.3398685	0.085845708
Axin2	axin2	223.7622736	0.582166117	202.2410415	0.521127278	429.3812343	0.249343351
Axin1	axin 1	164.4811794	0.357051665	192.2826903	0.48170679	341.4549736	0.332440932
Apc2	adenomatosis polyposis coli 2	98.85499999	0.124948223	94.26789929	0.114534278	863.1040594	0.101742905
Nuclear Factors							
Tcf4	transcription factor 4	986.4723963	0.251483716	1197.491493	0.248273344	3973.331888	0.889945086
Tcf3	transcription factor 3	190.5045881	0.48987916	179.8919114	0.57458275	331.552919	0.312585321
Lef1	lymphoid enhancer binding factor 1	234.9432668	0.648208795	173.6581248	0.553021659	424.8355608	0.207245367

doi:10.1371/journal.pone.0087038.t007

substrates of Type I receptors for BMPs, whereas SMAD2 and 3 are substrates for Type I receptors for TGFβs and Activins. Once activated, R-SMADs assemble with SMAD4, also known as co-SMAD, and the heterodimer translocates into the nucleus to regulate responsive gene expression.

In LE and IE cells, the *Acvr2a* was the significantly expressed receptor gene, while *Smad2* was the abundantly expressed gene for intracellular transmitter. In addition, expression of *Bmp7* was relatively abundant in LE, and *Growth differentiation factor 10* (*Gdf10*) was abundant in IE cells (Table 6). Furthermore, the IE cells had a slightly higher expression of *inhibin beta-B*, but much higher *Bmp5*, *Bmpr1a* and *Acvr1*.

Previous genetic studies in mice have implicated TGF β signaling in eyelid closure. Huang *et. al.* carried out a methodical gene knockout study, in which each TGFβ cascade was specifically inactivated in ocular surface epithelium [13]. The results showed that BMP, but not TGFβ or activin, signaling was required for eyelid closure. The EOB phenotype was observed in mice lacking the type I BMP receptor genes, *Acvr1* and *Bmpr1a*, the R-Smad genes, *Smad 1* and *Smad5*, and the Co-Smad gene, *Smad 4*, but not in mice lacking the type II TGFβ receptor gene *Tgfbr2* and the activin/TGFβ-activated R-Smad genes, *Smad2* and *Smad3*. Conditional deletion of *Bmpr1a* in the ectoderm and overexpression of the inhibitory SMAD7 in keratinocytes also led to an EOB phenotype [68,69]. Our data showed that although the LE and IE cells had type II BMP receptor expression, only the IE cells expressed abundantly the type I receptor BMPR1A. Hence, activation of the BMP pathway can be carried out mainly in the IE cells.

Of the ligands highly expressed in IE cells, BMP5 is required for chondrocytic activity during endochondral ossification, and its deficiency leads to a number of skeletal defects [70]. GDF10 is expressed in skeletal muscles but is dispensable for fetal development [71]. Recently, it was shown that GDF10, similar to TGFβ, can activate Smad2/3 and counteract the BMP signals [72]. Of the ligands highly expressed in LE cells, BMP7 is required for eye development, but is dispensable for eyelid closure [73]. The *inhibin βB* is required for embryonic eyelid closure; however, it may

Table 8. Expression of genes in the Shh pathways

		LE		IE		LE/IE	
symbol	**name**	**ave.int**	**p-val**	**ave.int**	**p-val**	**fold**	**p.val**
The SHH pathways							
Ligands							
Ihh	Indian hedgehog	147.1238905	0.343655971	163.4318248	0.257104942	-1.11084491	0.159752369
Shh	sonic hedgehog	114.5198084	0.921343416	90.82711316	0.707793588	1.260854875	0.057945482
Dhh	desert hedgehog	81.67346381	0.295695919	78.22022394	0.448188021	1.04414766	0.356208622
Receptors							
Ptch1	patched homolog 1	732.1286053	0.151756837	387.1397413	0.159961283	1.891122319	0.065360857
Smo	smoothened homolog (Drosophila)	232.128924	0.720827257	236.9900927	0.535847474	-1.020941676	0.043881503
Ptch2	patched homolog 2	177.2644254	0.916565611	129.2130979	0.724494389	**1.3718766**	**0.046898841**
Ptchd2	patched domain containing 2	62.24859935	0.381277507	81.98061543	0.279593571	-1.31698731	0.215221343
Ptchd1	patched domain containing 1	53.35715576	0.307765053	111.3612941	0.554778418	-2.087092023	0.350146107
Nuclear factors							
Gli2	GLI-Kruppel family member GLI2	323.275679	0.284969075	208.0211403	0.899972309	**1.554052047**	**0.014527635**
Gli1	GLI-Kruppel family member GLI1	254.0822594	0.875224653	194.1079797	0.351745286	1.308973798	0.095148044
Gli3	GLI-Kruppel family member GLI3	219.0576273	0.361664682	230.2743744	0.290554641	-1.05120455	0.513564801

doi:10.1371/journal.pone.0087038.t008

do so through a mechanism independent of SMAD [13,20,39]. These observations seem to support the idea that activation of the BMP pathways for eyelid closure is initiated by BMP4 produced by the the mesenchymal cells, but not ligands produced in the epithelial cells [13]. Collectively, the gene expression pattern has identified differential expression of *Bmpr1a*, *Inhbb* and *Bmp5* in the LE and IE cells, and suggests that the BMP pathways may be preferentially activated in the IE cells.

Expression of genes involved in the canonical Wnt pathways

The canonical Wnt pathway is activated by binding of ligands to the Frizzled (FZD) receptors, seven-transmembrane proteins with 10 family members (FZD 1–10), and co-receptors, such as the low-density lipoprotein-related receptor protein-5 or -6 (LRP5/6) [74,75]. The receptor signal is transduced by the Dishevelled (DVL), which are scaffold proteins that interact with diverse

Table 9. Expresison of genes in the Notch pathways

		LE		IE		LE/IE	
symbol	**name**	**ave.int**	**p-val**	**ave.int**	**p-val**	**fold**	**p.val**
The Notch pathway							
Ligands							
Jag1	jagged 1	291.2881266	0.105374112	197.9402992	0.311677556	1.471595869	0.091068921
Dlk2	delta-like 2 homolog (Drosophila)	197.9473027	0.274112696	249.333394	0.127067789	-1.259594804	0.478878354
Dlk1	delta-like 1 homolog (Drosophila)	160.8057089	0.417447523	228.2743744	0.183766506	-1.419566358	0.713116482
Jag2	jagged 2	123.4294683	0.652072473	136.4169347	0.855040508	-1.105221764	0.044310212
Cntn2	contactin 2	90.82785012	0.973262036	135.9033179	0.861637408	-1.49627364	0.478848975
Dll3	delta-like 3 (Drosophila)	82.77031667	0.925984883	94.41873989	0.524248856	-1.140731891	0.145970717
Dll1	delta-like 1 (Drosophila)	58.175215	0.566824074	86.88336375	0.411054244	-1.493477312	0.478850038
Dll4	delta-like 4 (Drosophila)	50.38482269	0.44226217	74.30942025	0.241923917	-1.474837387	1
Cntn1	contactin 1	39.8413045	0.276648487	96.92132086	0.562892733	-2.432684423	0.478853114
Cntn3	contactin 3	29.72792312	0.137186651	79.6325516	0.309575696	-2.678712242	0.072194119
Receptor							
Notch1	Notch gene homolog 1 (Drosophila)	270.8341937	0.165136399	174.4555076	0.868921425	**1.552454247**	**0.049764805**
Notch3	Notch gene homolog 3 (Drosophila)	170.0357029	0.942106713	161.7710801	0.837205225	1.051088382	0.134639977
Notch2	Notch gene homolog 2 (Drosophila)	129.2094217	0.481897644	216.7538874	0.218496242	-1.677539335	0.202460017
Notch4	Notch gene homolog 4 (Drosophila)	126.7584274	0.44882783	132.3657333	0.23400882	-1.044236158	0.478848306

doi:10.1371/journal.pone.0087038.t009

Table 10. Expression of genes in the PCP pathways

		LE		IE		LE/IE	
symbol	**name**	**ave.int**	**p-val**	**ave.int**	**p-val**	**fold**	**p.val**
Ligands							
Wnt5b	wingless-related MMTV integration site 5B	142.8377647	0.251818298	175.1915846	0.766909218	-1.226507465	0.479705404
Wnt11	wingless-related MMTV integration site 11	84.42137039	0.652672424	103.3922602	0.26497932	-1.224716677	0.30355669
Wnt5a	wingless-related MMTV integration site 5A	77.85246206	0.486496883	212.9173909	0.41319785	-2.734883204	0.113472971
Receptors/co-receptors							
Fzd3	frizzled homolog 3 (Drosophila)	621.1053146	0.147519425	813.2745816	0.09579658	-1.309398845	0.478857045
Fzd6	frizzled homolog 6 (Drosophila)	228.5769945	0.707784383	253.913148	0.843771153	-1.110842972	0.809625026
Ptk7	PTK7 protein tyrosine kinase 7	131.0165691	0.823649378	130.2743778	0.519053347	1.005697139	0.271910987
Ror2	receptor tyrosine kinase-like orphan receptor 2	117.9563668	0.737154026	147.612897	0.626132679	-1.251419496	0.347033389
Ror1	receptor tyrosine kinase-like orphan receptor 1	49.65911375	0.205977337	121.7021912	0.464979521	-2.450752379	0.254560774
PCP core molecules							
Nkd1	naked cuticle 1 homolog (Drosophila)	**497.1448806**	**0.019711524**	296.7290136	0.106660925	1.675417158	0.059347345
Dvl3	dishevelled 3, dsh homolog (Drosophila)	**413.3018893**	**0.042567398**	**402.3131688**	**0.02480151**	1.027313847	0.154874206
Nkd2	naked cuticle 2 homolog (Drosophila)	190.6089541	0.450452887	228.3393772	0.284509583	-1.19794675	0.254709977
Celsr1	cadherin, EGF LAG seven-pass G-type receptor 1	143.6045951	0.772719535	135.8743755	0.995259555	1.056892402	0.06910682
Scrib	scribbled homolog (Drosophila)	141.4973543	0.791394792	147.7381109	0.866894575	-1.044105111	0.121047968
Vangl1	vang-like 1 (van gogh, Drosophila)	131.9203286	0.88139334	183.465837	0.537481643	-1.390732111	0.345788803
Dvl2	dishevelled 2, dsh homolog (Drosophila)	113.9854854	0.927335626	168.4318283	0.660389528	-1.477660316	0.473187759
Celsr2	cadherin, EGF LAG seven-pass G-type receptor 2	112.3460222	0.908420016	106.673064	0.611755773	1.053180794	0.021674089
Dvl1	dishevelled, dsh homolog 1 (Drosophila)	107.1117074	0.846548722	145.3054246	0.894048687	**-1.35657836**	**0.026996352**
Ankrd6	ankyrin repeat domain 6	90.63533762	0.639562999	97.05578363	0.481777055	-1.07083822	0.479084068
Prickle3	prickle homolog 3 (Drosophila)	84.83043606	0.563803071	79.27375338	0.261432352	1.07009486	0.177745976
Prickle4	prickle homolog 4 (Drosophila)	80.8529364	0.511691571	106.7370389	0.612627926	-1.320138064	0.286671885
Celsr3	cadherin, EGF LAG seven-pass G-type receptor 3	79.55497285	0.494713944	86.50478832	0.346172204	-1.087358656	0.355310588
Vangl2	vang-like 2 (van gogh, Drosophila)	75.68020564	0.444286165	94.43627767	0.447152767	-1.247833259	0.215185176
Prickle2	prickle homolog 2 (Drosophila)	65.94364237	0.321422465	109.7444823	0.653633857	-1.664216266	1
Prickle1	prickle homolog 1 (Drosophila)	55.46965977	0.201923392	73.22103016	0.197860129	-1.320019457	0.912533584
COPII vesicle							
Sec24b	Sec24 related gene family, member B	365.8694535	0.189701062	**499.6743376**	**0.03653965**	-1.365717561	0.217269914
Sec24c	Sec24 related gene family, member C	334.7646094	0.254211948	299.8711063	0.603744187	1.116361671	0.170013082
Sec24a	Sec24 related gene family, member A	259.536154	0.51602466	329.3725376	0.968581141	-1.269081523	0.67083081
Sec23ip	Sec23 interacting protein	138.61087	0.575686004	308.2026826	0.704727443	-2.223510194	0.218337641
Sec23b	SEC23B (S. cerevisiae)	128.5699587	0.481018944	308.1660899	0.704276804	-2.396874767	0.326855537
Sec24d	Sec24 related gene family, member D	126.0420706	0.457514143	272.5389393	0.313682332	-2.162285481	0.165560621
Sec23a	SEC23A (S. cerevisiae)	105.0683677	0.274034086	347.439549	0.815321433	-3.30679496	0.243266726

doi:10.1371/journal.pone.0087038.t010

proteins, including kinases, phosphatases and adaptor proteins. Intracellular transduction of the Wnt signal is carried out by stabilization and cytosolic accumulation of the critical mediator, β-catenin. The β-catenin then translocates to the nucleus, binds with members of the T-cell factor (TCF)/lymphocyte enhancer factor (Lef) family of transcription factors to regulate target gene expression [76].

Wnt ligands are a family of secreted signaling proteins, consisting of 19 members in mammals [77]. Their activities are antagonized by the Secreted frizzled-related proteins (SFRPs) and the dickkopf homologs (DKKs). The SFRP is a family of secreted glycoproteins that may antagonize Wnt-mediated signaling by direct competitive interaction with Wnt ligands or by formation of non-signaling complexes with Frizzled proteins [78,79]. The DKKs, also secreted cysteine-rich proteins, interact with and inhibit the Wnt co-receptor Lrp5/6 [80].

The array data showed that the *Fzd3* was the most abundant receptor and *Ctnnb1* and *Tcf4* were abundant intracellular transducers expressed in LE and IE cells. While *Sfrp2* was highly expressed in LE and IE cells, *Dkk2* and *Sfrp1* were abundantly expressed in the IE cells, and *Apcdd1* was abundant in the LE cells (Table 7). In addition, *Dkk2* was 4-fold more abundant in the IE cells, conversely, *Apcdd1* was 1.7-fold more abundant in the LE cells.

Among the receptors highly expressed, FZD9 is required for bone morphogenesis and is a receptor for non-canonical Wnt that activates JNK, while DVL3 is required for cardiac outflow tract development [81–84]. Neither, however, is known to be involved

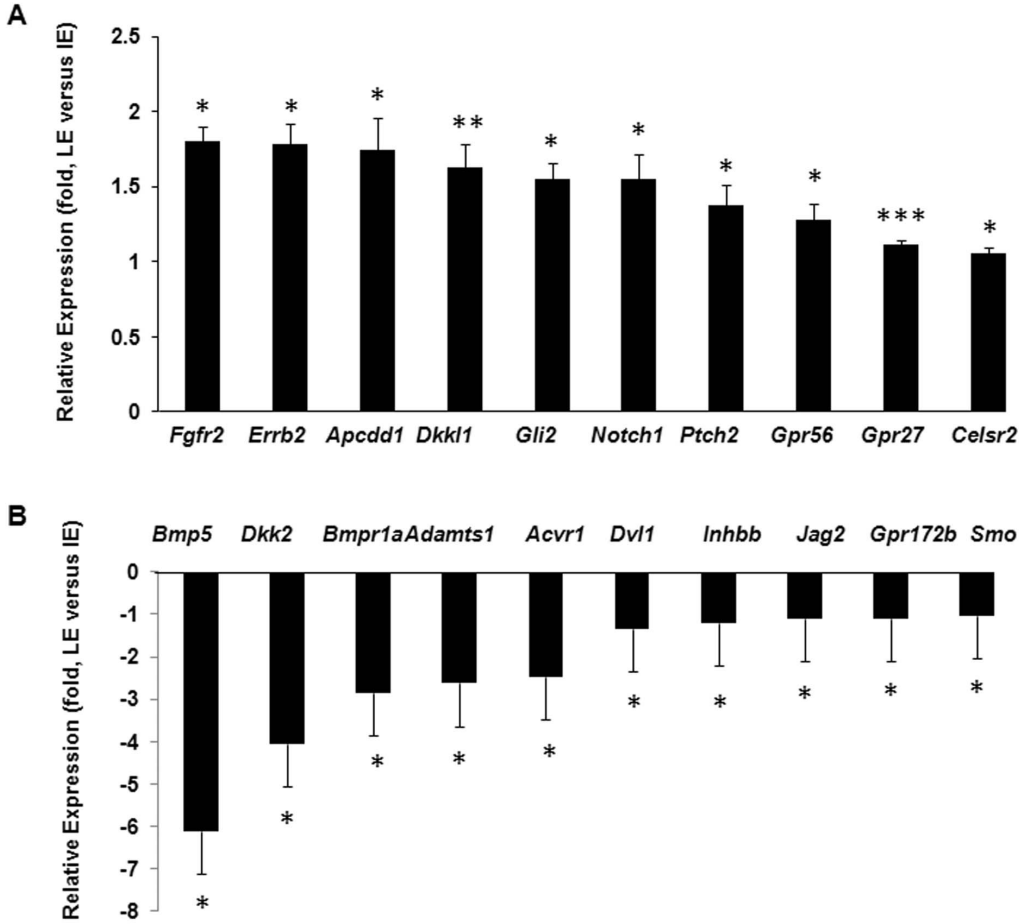

Figure 1. Summary of the microarray analyses. Genes differentially expressed in LE and IE cells. Statistical significant differential gene expression between LE and IE samples were summarized in (A) genes expressed more in LE than IE cells, and (B) genes expressed less in LE than IE cells. * $p<0.05$, ** $p<0.01$ and *** $p<0.001$ are considered significant.
doi:10.1371/journal.pone.0087038.g001

in eyelid closure. Conversely, FZD3, involved in axonal outgrowth, and FZD6, required for hair patterning, can collaborate on eyelid closure. Knocking out both *Fzd3* and *Fzd6* causes "unfused eyelids" in 10% of the offsprings [85,86]. Likewise, the *Lrp6(−/−)* mice display multiple defects, including open eyes [87–89]. Although the nuclear factor TCF4 has not been implicated in eyelid closure, TCF3, through interactions with β-catenin, is shown to be crucial for eyelid closure [36,90].

Using the Wnt reporter mice, it was shown that Wnt activity is repressed overall in eyelid epithelium [36]. The repression is likely to be mediated by the expression of Wnt antagonists. On the one hand, the retinoic acid (RA)-Pitx2 pathway can induce the expression of Wnt antagonists in the periocular mesenchyme; while on the other hand, the BMP and FGFR2 pathways can activate the expression of Wnt antagonists in ocular surface epithelium [13,91]. Our results showed that antagonists could indeed be produced in the LE and IE cells. Of the antagonists, SFRP4 is dispensable for fetal development; SFRP1 and SFRP2 have redundant functions in regulating embryonic patterning, and DKK2 is required for epithelial differentiation and eyelid closure [12,92–94]. In addition, APCDD1 is a membrane-bound glycoprotein that can interact with WNT3A and LRP5 and inhibit Wnt signaling in a cell-autonomous manner [95]. Our data also suggested that the LE and IE cells might use distinct antagonists for Wnt inhibition.

In the Wnt reporter mice, it is also shown that the canonical Wnt pathway is activated in restricted areas of the developing eyelids [36]. Specifically, Wnt activity is induced in a small group of epithelial cells positioned at the transition zone between the palpebral conjunctiva and eyelid tip epidermis, so called mucocutaneous junction (MCJ) [96,97]. Repression of Wnt in the MCJ cells results in failure of eyelid closure [36]. Hence, Wnt may establish distinct morphogenetic fields within the developing eyelids, so that activation takes place in MCJ, but repression occurs elsewhere. Isolation of the MCJ cells and characterizing their molecular signatures may help to understand the developmental roles of the temporal-spatial Wnt activity.

Genes in the SHH, NOTCH and the PCP pathways

The Sonic Hedgehog ligands bind to the transmembrane receptor Patched (*Ptch*) to initiate pathway signaling [98]. In its inactive state, PTCH exerts an inhibitory effect on the signal transducer Smoothened (SMO), but upon ligand binding, the inhibition on SMO is released and downstream signaling occurs. This leads to the activation of the Gli transcription factors. We found that expression of *Ptch1*, *Smo* and *Gli2*, but not the ligand genes, was relatively abundant in IE and LE cells (Table 8). This is in agreement with the idea that activation of Shh pathway is dependent on *Ptch1* expression induced by the FGFR signaling in the eyelid epithelial cells, and the SHH expression induced by

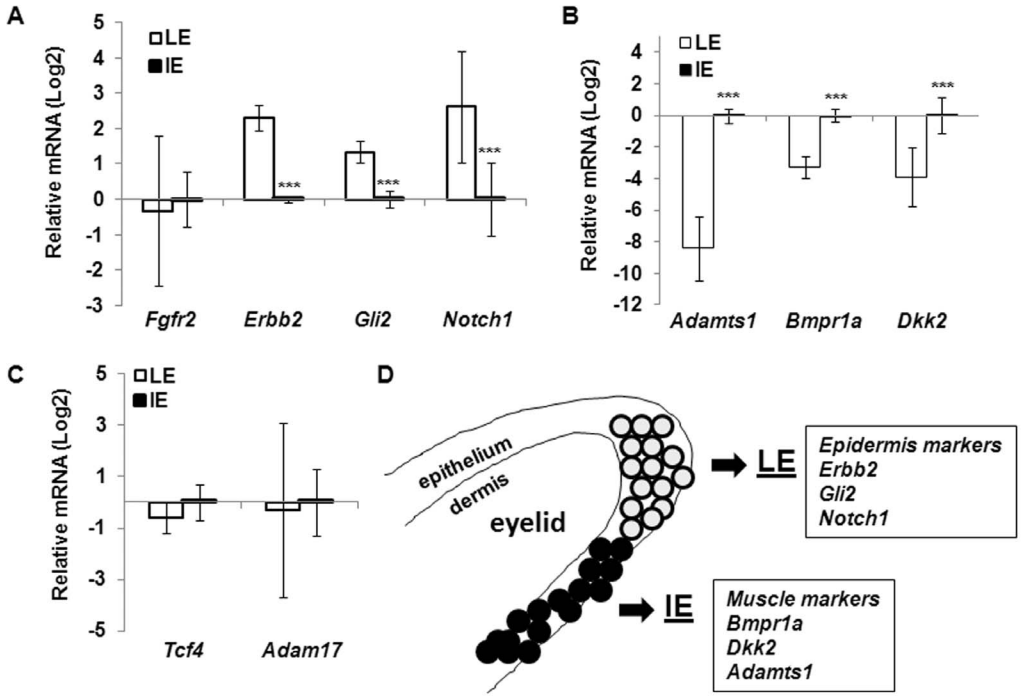

Figure 2. Differential gene expression in LE and IE cells. Total RNA isolated from LE and IE cells of fetuses at E15.5 was used for qRT-PCR for the expression of (A) *Fgfr2*, *Errb2*, *Gli2* and *Notch1*, (B) *Adamts1*, *Bmpr1a* and *Dkk2* and (C) *Tcf4* and *Adam17*. Relative expression was calculated based on that of *Gapdh* in each sample, and compared to the expression in IE cells, set as 1. The results are shown as mean ± SD from at least 3 samples and triplicate PCR of each sample. Statistic analyses were done by Student t-test, ***$p<0.001$ is considered significant. (D) Figure depicting the LE and IE cells in the developing eyelid and expresison of signaling factors.
doi:10.1371/journal.pone.0087038.g002

FGF10 in the periocular mesenchyme [6,13]. Furthermore, many of the genes were expressed slightly but significantly higher in LE than in IE cells, suggesting that this pathway may be differentially activated in these cells.

The NOTCH cascade consists of NOTCH, its ligands, and intracellular signal transmitters. Mammals possess four different notch receptors, including NOTCH 1–4, which are membrane-tethered transcription factors. They are activated by the ligands of the Delta, Serrate, Lag-2 families. In LE and IE cells, expression of NOTCH ligands and receptors was overall low, but *Jag1* was 1.5-fold and *Notch 1* was 1.5-fold more abundant in the LE than in the IE cells (Table 9). The role of NOTCH in eyelid development however has been inconclusive. On the one hand, constitutive activation of NOTCH in periocular mesenchyme leads to abnormalities in cranial facial development and incomplete eyelid closure; on the other hand, genetic ablation of NOTCH signaling in ocular surface epithelium does not cause an EOB phenotype [12,13,99–101].

The non-canonical Wnt/planar cell polarity (PCP) pathway regulates cell orientation within the plane of a cell sheet and is involved in convergent extension during development [28,102]. WNT5A, WNT5B, and WNT11 are the non-canonical WNT ligands, and FZD 3/6 and DVL are the receptors, which transmit signals through the core PCP proteins. The core is composed of cytoplasmic Prickled (PK), the transmembrane protein Van Gogh, the cadherin Starry/Flamingo (STAN/FMI), and the Ankyrin repeat protein Diego (DGO) [103,104]. In addition, SEC24B is a cargo-binding component of the COPII vesicle coat [105]. The COPII vesicles are the primary pathway for active transport of secretary proteins from the ER to the Golgi. Though SEC24B is not a PCP core component, it selectively sorts VANGL2 into COPII vesicles thereby controlling PCP assembly and activity.

Expression of non-canonical Wnt ligands and core receptors was overall low in LE and IE cells with a few exceptions (Table 10). While expression of *Fzd3* and *Dvl3* was relatively abundant in LE and IE cells, expression of *naked cuticle 1 homolog* (*Nkd1*) was higher in LE, and expression of *Sec24b* was higher in IE cells. Genetic inactivation of many PCP genes, including *Fzd3/6*, *Dvl2*, *Vangl2*, *Scrb1*, *Ptk7* and *Celsr1*, as well as *Sec24b*, causes craniofacial developmental abnormalities, including open eyelids [27–33,35,106]. It is yet to be determined whether the eyelid defect is secondary to craniofacial abnormalities resulting from inactivation of the PCP pathways.

Validation of differential gene expression by qRT-PCR

Collectively, the microarray studies identified 20 genes of the morphogenetic signaling pathways were differentially expressed in the LE and IE cells (Fig. 1). To validate the results, we used qRT-PCR to examine 7 relatively abundant genes (Fig. 2A and 2B). Consistent with the array data, qRT-PCR showed that the LE cells had significantly more expression of *Erbb2*, *Gli2* and *Notch1*, but significantly less expression of *Adamts1*, *Bmpr1a* and *Dkk2* than the IE cells. Also consistent with the array data, qRT-PCR showed that the LE cells had a slight but insignificant decrease in expression of *Tcf4* and *Adam17* than the IE cells (Fig. 2C, Tables 4 and 7). Different from the array data, however, qRT-PCR detected no difference of *Fgfr2* expression in LE and IE cells (Fig. 2A). Hence, most gene expression pattern observed by cDNA array can be validated by qRT-PCR.

Conclusions

The LE and IE cells have the same ontogenic origin, but different developmental fate. The fate divergence can be detected at E15.5, as the IE cells develop gene expression signatures towards the muscle lineage, while the LE cells express epidermal markers. The LE cells also undergo morphological changes and migrate at E15.5 to eventually form the closed eyelid. This morphogenetic event is thought to be dictated by specific activation of signaling pathways. Our results show that the LE and IE cells are overall quite similar in the compositions for the major "eyelid closure pathways", but there are a few differences (Fig. 2D). The LE cells have a slight but significant increased expression of *Erbb2* of the EGF pathway, *Pach1*and *2* and *Gli2* of the Shh pathway, *Jag1* and *Notch 1* of the Notch pathway, and *Nkd1* of the PCP pathway, but the IE cells have higher expression of *Bmpr1a*, *Acvr1* and *Bmp5* of the BMP pathway. In addition, we find higher expression of *Apcdd1* in the LE cells, but higher expression of *Dkk2* in the IE cells of the Wnt pathway. Differential expression of signaling molecules in the eyelid epithelium may be one of the mechanisms for ectopic activation of morphogenetic pathways. The contributions of the eyelid mesenchyme should also be crucial and can be evaluated using the similar approach. Combination of LCM, cDNA array and pathway analyses can serve as a preliminary screening tool for identifying critical developmental genes for further expression and knockout studie.

Author Contributions

Conceived and designed the experiments: YX MM. Performed the experiments: QM CJ. Analyzed the data: YC JC MM. Contributed reagents/materials/analysis tools: MM. Wrote the paper: QM YX MM.

References

1. Pearson AA (1980) The development of the eyelids. Part I. External features. J Anat 130: 33–42.
2. Byun TH, Kim JT, Park HW, Kim WK (2011) Timetable for upper eyelid development in staged human embryos and fetuses. Anat Rec (Hoboken) 294: 789–796.
3. Harris MJ, McLeod MJ (1982) Eyelid growth and fusion in fetal mice. A scanning electron microscope study. Anat Embryol (Berl) 164: 207–220.
4. Findlater GS, McDougall RD, Kaufman MH (1993) Eyelid development, fusion and subsequent reopening in the mouse. J Anat 183: 121–9.
5. Li C, Guo H, Xu X, Weinberg W, Deng CX (2001) Fibroblast growth factor receptor 2 (Fgfr2) plays an important role in eyelid and skin formation and patterning. Dev Dyn 222: 471–483.
6. Tao H, Ono K, Kurose H, Noji S, Ohuchi H (2006) Exogenous FGF10 can rescue an eye-open at birth phenotype of Fgf10-null mice by activating activin and TGFalpha-EGFR signaling. Dev Growth Differ 48: 339–346.
7. Harris MJ, Juriloff DM (1986) Eyelid development and fusion induced by cortisone treatment in mutant, lidgap-Miller, foetal mice. A scanning electron microscope study. J Embryol Exp Morphol 91: 1–18.
8. Juriloff DM, Harris MJ (1989) A scanning electron microscope study of fetal eyelid closure accelerated by cortisone in SWV/Bc mice. Teratology 40: 59–66.
9. Mohamed YH, Gong H, Amemiya T (2003) Role of apoptosis in eyelid development. Exp Eye Res 76: 115–123.
10. Matt N, Dupe V, Garnier JM, Dennefeld C, Chambon P, et al. (2005) Retinoic acid-dependent eye morphogenesis is orchestrated by neural crest cells. Development 132: 4789–4800.
11. Molotkov A, Molotkova N, Duester G (2006) Retinoic acid guides eye morphogenetic movements via paracrine signaling but is unnecessary for retinal dorsoventral patterning. Development 133: 1901–1910.
12. Gage PJ, Qian M, Wu D, Rosenberg KI (2008) The canonical Wnt signaling antagonist DKK2 is an essential effector of PITX2 function during normal eye development. Dev Biol 317: 310–324.
13. Huang J, Dattilo LK, Rajagopal R, Liu Y, Kaartinen V, et al. (2009) FGF-regulated BMP signaling is required for eyelid closure and to specify conjunctival epithelial cell fate. Development 136: 1741–1750.
14. Schaeper U, Vogel R, Chmielowiec J, Huelsken J, Rosario M, et al. (2007) Distinct requirements for Gab1 in Met and EGF receptor signaling in vivo. Proc Natl Acad Sci U S A 104: 15376–15381.
15. Qu CK, Yu WM, Azzarelli B, Feng GS (1999) Genetic evidence that Shp-2 tyrosine phosphatase is a signal enhancer of the epidermal growth factor receptor in mammals. Proc Natl Acad Sci U S A 96: 8528–33.
16. Crotty T, Cai J, Sakane F, Taketomi A, Prescott SM, et al. (2006) Diacylglycerol kinase delta regulates protein kinase C and epidermal growth factor receptor signaling. Proc Natl Acad Sci U S A 103: 15485–15490.
17. Wojnowski L, Stancato LF, Zimmer AM, Hahn H, Beck TW, et al. (1998) Craf-1 protein kinase is essential for mouse development. Mech Dev 76: 141–149.
18. Scholl FA, Dumesic PA, Barragan DI, Harada K, Bissonauth V, et al. (2007) Mek1/2 MAPK kinases are essential for Mammalian development, homeostasis, and Raf-induced hyperplasia. Dev Cell 12: 615–629.
19. Schwartzberg PL, Stall AM, Hardin JD, Bowdish KS, Humaran T, et al. (1991) Mice homozygous for the ablm1 mutation show poor viability and depletion of selected B and T cell populations. Cell 65: 1165–1175.
20. Zhang L, Wang W, Hayashi Y, Jester JV, Birk DE, et al. (2003) A role for MEK kinase 1 in TGF-beta/activin-induced epithelium movement and embryonic eyelid closure. Embo J 22: 4443–4454.
21. Takatori A, Geh E, Chen L, Zhang L, Meller J, et al. (2008) Differential transmission of MEKK1 morphogenetic signals by JNK1 and JNK2. Development 135: 23–32.
22. Weston CR, Wong A, Hall JP, Goad ME, Flavell RA, et al. (2003) JNK initiates a cytokine cascade that causes Pax2 expression and closure of the optic fissure. Genes Dev 17: 1271–1280.
23. Schramek D, Kotsinas A, Meixner A, Wada T, Elling U, et al. (2011) The stress kinase MKK7 couples oncogenic stress to p53 stability and tumor suppression. Nat Genet 43: 212–219.
24. Thumkeo D, Shimizu Y, Sakamoto S, Yamada S, Narumiya S (2005) ROCK-I and ROCK-II cooperatively regulate closure of eyelid and ventral body wall in mouse embryo. Genes Cells 10: 825–834.
25. Rice DS, Hansen GM, Liu F, Crist MJ, Newhouse MM, et al. (2012) Keratinocyte migration in the developing eyelid requires LIMK2. PLoS ONE 7: e47168.
26. Shimizu Y, Thumkeo D, Keel J, Ishizaki T, Oshima H, et al. (2005) ROCK-I regulates closure of the eyelids and ventral body wall by inducing assembly of actomyosin bundles. J Cell Biol 168: 941–953.
27. Kibar Z, Vogan KJ, Groulx N, Justice MJ, Underhill DA, et al. (2001) Ltap, a mammalian homolog of Drosophila Strabismus/Van Gogh, is altered in the mouse neural tube mutant Loop-tail. Nat Genet 28: 251–255.
28. Murdoch JN, Doudney K, Paternotte C, Copp AJ, Stanier P (2001) Severe neural tube defects in the loop-tail mouse result from mutation of Lpp1, a novel gene involved in floor plate specification. Hum Mol Genet 10: 2593–2601.
29. Hamblet NS, Lijam N, Ruiz-Lozano P, Wang J, Yang Y, et al. (2002) Dishevelled 2 is essential for cardiac outflow tract development, somite segmentation and neural tube closure. Development 129: 5827–5838.
30. Curtin JA, Quint E, Tsipouri V, Arkell RM, Cattanach B, et al. (2003) Mutation of Celsr1 disrupts planar polarity of inner ear hair cells and causes severe neural tube defects in the mouse. Curr Biol 13: 1129–1133.
31. Lu X, Borchers AG, Jolicoeur C, Rayburn H, Baker JC, et al. (2004) PTK7/CCK-4 is a novel regulator of planar cell polarity in vertebrates. Nature 430: 93–98.
32. Montcouquiol M, Rachel RA, Lanford PJ, Copeland NG, Jenkins NA, et al. (2003) Identification of Vangl2 and Scrb1 as planar polarity genes in mammals. Nature 423: 173–177.
33. Harris MJ, Juriloff DM (2007) Mouse mutants with neural tube closure defects and their role in understanding human neural tube defects. Birth Defects Res A Clin Mol Teratol 79: 187–210.
34. Rivera C, Simonson SJ, Yamben IF, Shatadal S, Nguyen MM, et al. (2013) Requirement for Dlgh-1 in planar cell polarity and skeletogenesis during vertebrate development. PLoS ONE 8: e54410.
35. Torban E, Patenaude AM, Leclerc S, Rakowiecki S, Gauthier S, et al. (2008) Genetic interaction between members of the Vangl family causes neural tube defects in mice. Proc Natl Acad Sci U S A 105: 3449–3454.
36. Wu CI, Hoffman JA, Shy BR, Ford EM, Fuchs E, et al. (2012) Function of Wnt/beta-catenin in counteracting Tcf3 repression through the Tcf3-beta-catenin interaction. Development 139: 2118–2129.
37. Luetteke NC, Qiu TH, Fenton SE, Troyer KL, Riedel RF, et al. (1999) Targeted inactivation of the EGF and amphiregulin genes reveals distinct roles for EGF receptor ligands in mouse mammary gland development. Development 126: 2739–2750.
38. Luetteke NC, Qiu TH, Peiffer RL, Oliver P, Smithies O, et al. (1993) TGF alpha deficiency results in hair follicle and eye abnormalities in targeted and waved-1 mice. Cell 73: 263–78.
39. Vassalli A, Matzuk MM, Gardner HA, Lee KF, Jaenisch R (1994) Activin/inhibin beta B subunit gene disruption leads to defects in eyelid development and female reproduction. Genes Dev 8: 414–27.
40. Jin C, Chen J, Meng Q, Carreira V, Tam NN, et al. (2012) Deciphering gene expression program of MAP3K1 in mouse eyelid morphogenesis. Dev Biol.
41. Schnekenburger M, Peng L, Puga A (2007) HDAC1 bound to the Cyp1a1 promoter blocks histone acetylation associated with Ah receptor-mediated trans-activation Biochim Biophys Acta 1769: 569–578.

42. Smyth GK (2004) Linear models and empirical bayes methods for assessing differential expression in microarray experiments. Stat Appl Genet Mol Biol 3: Article3.
43. Dai M, Wang P, Boyd AD, Kostov G, Athey B, et al. (2005) Evolving gene/transcript definitions significantly alter the interpretation of GeneChip data. Nucleic Acids Res 33: e175.
44. Kauffmann A, Gentleman R, Huber W (2009) arrayQualityMetrics–a bioconductor package for quality assessment of microarray data. Bioinformatics 25: 415–416.
45. Sartor MA, Leikauf GD, Medvedovic M (2009) LRpath: a logistic regression approach for identifying enriched biological groups in gene expression data. Bioinformatics 25: 211–217.
46. Freudenberg JM, Joshi VK, Hu Z, Medvedovic M (2009) CLEAN: CLustering Enrichment ANalysis. BMC Bioinformatics 10: 234.
47. Ashburner M, Ball CA, Blake JA, Botstein D, Butler H, et al. (2000) Gene ontology: tool for the unification of biology. The Gene Ontology Consortium. Nat Genet 25: 25–29.
48. Reuss B, von Bohlen und HO (2003) Fibroblast growth factors and their receptors in the central nervous system. Cell Tissue Res 313: 139–157.
49. Goetz R, Mohammadi M (2013) Exploring mechanisms of FGF signalling through the lens of structural biology. Nat Rev Mol Cell Biol 14: 166–180.
50. Al AD, Sala FG, Baptista S, Galzote R, Danopoulos S, et al. (2012) FGF9-Pitx2-FGF10 signaling controls cecal formation in mice. Dev Biol 369: 340–348.
51. Okada K, Noda M, Nogawa H (2013) Autocrine growth factors are involved in branching morphogenesis of mouse lung epithelium. Zoolog Sci 30: 1–6.
52. Colvin JS, Green RP, Schmahl J, Capel B, Ornitz DM (2001) Male-to-female sex reversal in mice lacking fibroblast growth factor 9. Cell 104: 875–889.
53. Colvin JS, White AC, Pratt SJ, Ornitz DM (2001) Lung hypoplasia and neonatal death in Fgf9-null mice identify this gene as an essential regulator of lung mesenchyme. Development 128: 2095–2106.
54. Pirvola U, Zhang X, Mantela J, Ornitz DM, Ylikoski J (2004) Fgf9 signaling regulates inner ear morphogenesis through epithelial-mesenchymal interactions. Dev Biol 273: 350–360.
55. Zenz R, Scheuch H, Martin P, Frank C, Eferl R, et al. (2003) c-Jun Regulates Eyelid Closure and Skin Tumor Development through EGFR Signaling. Dev Cell 4: 879–889.
56. Li G, Gustafson-Brown C, Hanks SK, Nason K, Arbeit JM, et al. (2003) c-Jun Is Essential for Organization of the Epidermal Leading Edge. Dev Cell 4: 865–877.
57. Hynes NE, Lane HA (2005) ERBB receptors and cancer: the complexity of targeted inhibitors. Nat Rev Cancer 5: 341–354.
58. Dhomen NS, Mariadason J, Tebbutt N, Scott AM (2012) Therapeutic targeting of the epidermal growth factor receptor in human cancer. Crit Rev Oncog 17: 31–50.
59. Miettinen PJ, Berger JE, Meneses J, Phung Y, Pedersen RA, et al. (1995) Epithelial immaturity and multiorgan failure in mice lacking epidermal growth factor receptor. Nature 376: 337–41.
60. Saftig P, Reiss K (2011) The "A Disintegrin And Metalloproteases" ADAM10 and ADAM17: novel drug targets with therapeutic potential? Eur J Cell Biol 90: 527–535.
61. Hassemer EL, Endres B, Toonen JA, Ronchetti A, Dubielzig R, et al. (2012) ADAM17 Transactivates EGFR Signaling During Embryonic Eyelid Closure. Invest Ophthalmol Vis Sci.
62. Le Gall SM, Bobe P, Reiss K, Horiuchi K, Niu XD, et al. (2009) ADAMs 10 and 17 represent differentially regulated components of a general shedding machinery for membrane proteins such as transforming growth factor alpha, L-selectin, and tumor necrosis factor alpha. Mol Biol Cell 20: 1785–1794.
63. Scheller J, Chalaris A, Garbers C, Rose-John S (2011) ADAM17: a molecular switch to control inflammation and tissue regeneration. Trends Immunol 32: 380–387.
64. Kato S, Mohri Y, Matsuo T, Ogawa E, Umezawa A, et al. (2007) Eye-open at birth phenotype with reduced keratinocyte motility in LGR4 null mice. FEBS Lett 581: 4685–4690.
65. Wang Z, Jin C, Li H, Li C, Hou Q, et al. (2010) GPR48-Induced keratinocyte proliferation occurs through HB-EGF mediated EGFR transactivation. FEBS Lett 584: 4057–4062.
66. Mann GB, Fowler KJ, Gabriel A, Nice EC, Williams RL, et al. (1993) Mice with a null mutation of the TGF alpha gene have abnormal skin architecture, wavy hair, and curly whiskers and often develop corneal inflammation. Cell 73: 249–61.
67. Mueller TD, Nickel J (2012) Promiscuity and specificity in BMP receptor activation. FEBS Lett 586: 1846–1859.
68. He W, Li AG, Wang D, Han S, Zheng B, et al. (2002) Overexpression of Smad7 results in severe pathological alterations in multiple epithelial tissues EMBO J 21: 2580–2590.
69. Andl T, Ahn K, Kairo A, Chu EY, Wine-Lee L, et al. (2004) Epithelial Bmpr1a regulates differentiation and proliferation in postnatal hair follicles and is essential for tooth development. Development 131: 2257–2268.
70. Bailon-Plaza A, Lee AO, Veson EC, Farnum CE, van der Meulen MC (1999) BMP-5 deficiency alters chondrocytic activity in the mouse proximal tibial growth plate. Bone 24: 211–216.
71. Zhao R, Lawler AM, Lee SJ (1999) Characterization of GDF-10 expression patterns and null mice. Dev Biol 212: 68–79.
72. Matsumoto Y, Otsuka F, Hino J, Miyoshi T, Takano M, et al. (2012) Bone morphogenetic protein-3b (BMP-3b) inhibits osteoblast differentiation via Smad2/3 pathway by counteracting Smad1/5/8 signaling. Mol Cell Endocrinol 350: 78–86.
73. Dudley AT, Lyons KM, Robertson EJ (1995) A requirement for bone morphogenetic protein-7 during development of the mammalian kidney and eye. Genes Dev 9: 2795–2807.
74. Bhanot P, Brink M, Samos CH, Hsieh JC, Wang Y, et al. (1996) A new member of the frizzled family from Drosophila functions as a Wingless receptor. Nature 382: 225–230.
75. Wehrli M, Dougan ST, Caldwell K, O'Keefe L, Schwartz S, et al. (2000) arrow encodes an LDL-receptor-related protein essential for Wingless signalling. Nature 407: 527–530.
76. van de WM, Cavallo R, Dooijes D, van BM, van EJ, et al. (1997) Armadillo coactivates transcription driven by the product of the Drosophila segment polarity gene dTCF. Cell 88: 789–799.
77. Takada R, Satomi Y, Kurata T, Ueno N, Norioka S, et al. (2006) Monounsaturated fatty acid modification of Wnt protein: its role in Wnt secretion. Dev Cell 11: 791–801.
78. Dann CE, Hsieh JC, Rattner A, Sharma D, Nathans J, et al. (2001) Insights into Wnt binding and signalling from the structures of two Frizzled cysteine-rich domains. Nature 412: 86–90.
79. Bafico A, Gazit A, Pramila T, Finch PW, Yaniv A, et al. (1999) Interaction of frizzled related protein (FRP) with Wnt ligands and the frizzled receptor suggests alternative mechanisms for FRP inhibition of Wnt signaling. J Biol Chem 274: 16180–16187.
80. He X, Semenov M, Tamai K, Zeng X (2004) LDL receptor-related proteins 5 and 6 in Wnt/beta-catenin signaling: arrows point the way. Development 131: 1663–1677.
81. Ranheim EA, Kwan HC, Reya T, Wang YK, Weissman IL, et al. (2005) Frizzled 9 knock-out mice have abnormal B-cell development. Blood 105: 2487–2494.
82. Heasley LE, Winn RA (2008) Analysis of Wnt7a-stimulated JNK activity and cJun phosphorylation in non-small cell lung cancer cells. Methods Mol Biol 468: 187–196.
83. Albers J, Schulze J, Beil FT, Gebauer M, Baranowsky A, et al. (2011) Control of bone formation by the serpentine receptor Frizzled-9. J Cell Biol 192: 1057–1072.
84. Etheridge SL, Ray S, Li S, Hamblet NS, Lijam N, et al. (2008) Murine dishevelled 3 functions in redundant pathways with dishevelled 1 and 2 in normal cardiac outflow tract, cochlea, and neural tube development. PLoS Genet 4: e1000259.
85. Wang Y, Thekdi N, Smallwood PM, Macke JP, Nathans J (2002) Frizzled-3 is required for the development of major fiber tracts in the rostral CNS. J Neurosci 22: 8563–8573.
86. Guo N, Hawkins C, Nathans J (2004) Frizzled6 controls hair patterning in mice. Proc Natl Acad Sci U S A 101: 9277–9281.
87. Kato M, Patel MS, Levasseur R, Lobov I, Chang BH, et al. (2002) Cbfa1-independent decrease in osteoblast proliferation, osteopenia, and persistent embryonic eye vascularization in mice deficient in Lrp5, a Wnt coreceptor. J Cell Biol 157: 303–314.
88. Zhou CJ, Molotkov A, Song L, Li Y, Pleasure DE, et al. (2008) Ocular coloboma and dorsoventral neuroretinal patterning defects in Lrp6 mutant eyes. Dev Dyn 237: 3681–3689.
89. Zhou CJ, Wang YZ, Yamagami T, Zhao T, Song L, et al. (2010) Generation of Lrp6 conditional gene-targeting mouse line for modeling and dissecting multiple birth defects/congenital anomalies. Dev Dyn 239: 318–326.
90. Korinek V, Barker N, Moerer P, van DE, Huls G, et al. (1998) Depletion of epithelial stem-cell compartments in the small intestine of mice lacking Tcf-4. Nat Genet 19: 379–383.
91. Kumar S, Duester G (2010) Retinoic acid signaling in perioptic mesenchyme represses Wnt signaling via induction of Pitx2 and Dkk2. Dev Biol 340: 67–74.
92. Satoh W, Gotoh T, Tsunematsu Y, Aizawa S, Shimono A (2006) Sfrp1 and Sfrp2 regulate anteroposterior axis elongation and somite segmentation during mouse embryogenesis. Development 133: 989–999.
93. Christov M, Koren S, Yuan Q, Baron R, Lanske B (2011) Genetic ablation of sfrp4 in mice does not affect serum phosphate homeostasis. Endocrinology 152: 2031–2036.
94. Mukhopadhyay M, Gorivodsky M, Shtrom S, Grinberg A, Niehrs C, et al. (2006) Dkk2 plays an essential role in the corneal fate of the ocular surface epithelium. Development 133: 2149–2154.
95. Shimomura Y, Agalliu D, Vonica A, Luria V, Wajid M, et al. (2010) APCDD1 is a novel Wnt inhibitor mutated in hereditary hypotrichosis simplex. Nature 464: 1043–1047.
96. Knop E, Korb DR, Blackie CA, Knop N (2010) The lid margin is an underestimated structure for preservation of ocular surface health and development of dry eye disease. Dev Ophthalmol 45: 108–122.
97. Riau AK, Barathi VA, Beuerman RW (2008) Mucocutaneous junction of eyelid and lip: a study of the transition zone using epithelial cell markers. Curr Eye Res 33: 912–922.
98. Rubin LL, de Sauvage FJ (2006) Targeting the Hedgehog pathway in cancer. Nat Rev Drug Discov 5: 1026–1033.

99. Zhang Y, Lam O, Nguyen MT, Ng G, Pear WS, et al. (2013) Mastermind-like transcriptional co-activator-mediated Notch signaling is indispensable for maintaining conjunctival epithelial identity. Development 140: 594–605.
100. Saravanamuthu SS, Le TT, Gao CY, Cojocaru RI, Pandiyan P, et al. (2012) Conditional ablation of the Notch2 receptor in the ocular lens. Dev Biol 362: 219–229.
101. Zhang Y, Kao WW, Pelosi E, Schlessinger D, Liu CY (2011) Notch gain of function in mouse periocular mesenchyme downregulates FoxL2 and impairs eyelid levator muscle formation, leading to congenital blepharophimosis. J Cell Sci 124: 2561–2572.
102. Wang Y, Nathans J (2007) Tissue/planar cell polarity in vertebrates: new insights and new questions. Development 134: 647–658.
103. Adler PN (2002) Planar signaling and morphogenesis in Drosophila. Dev Cell 2: 525–535.
104. Seifert JR, Mlodzik M (2007) Frizzled/PCP signalling: a conserved mechanism regulating cell polarity and directed motility. Nat Rev Genet 8: 126–138.
105. Miller EA, Beilharz TH, Malkus PN, Lee MC, Hamamoto S, et al. (2003) Multiple cargo binding sites on the COPII subunit Sec24p ensure capture of diverse membrane proteins into transport vesicles. Cell 114: 497–509.
106. Merte J, Jensen D, Wright K, Sarsfield S, Wang Y, et al. (2010) Sec24b selectively sorts Vangl2 to regulate planar cell polarity during neural tube closure. Nat Cell Biol 12: 41–46.